BMC Plant Biology

RESEARCH Open Access

Study on the physiological mechanism and transcriptional regulatory network of early fruit development in *Gleditsia sinensis* Lam. (Fabaceae)

Qiao Liu[1,2,3,4], Yang Zhao[1,2,3,4], Ju Yang[1,2,3,4], Feng Xiao[1,2,3,4] and Xiurong Wang[1,2*]

Abstract

Background *Gleditsia sinensis Lam.* (Fabaceae) is a medicinal legume characterized by its spines and pods, which are rich in saponins, polysaccharides, and various specialized metabolites with potential medicinal and industrial applications. The low fruit set rate in artificially cultivated economic forests significantly impedes its development and utilization. A comprehensive understanding of the cellular events, physiological and biochemical processes, and molecular regulatory mechanisms underlying fruit initiation and early fruit development is essential for enhancing yield. However, such information for *G. sinensis* remains largely unexplored.

Results In this study, we identified that the early fruit development process in *G. sinensis* can be categorized into three distinct stages: pollination, the critical period of fertilization, and the initial fruit development followed by subsequent growth. The dynamic changes in non-structural carbohydrates and endogenous plant hormones within the ovary were found to play a significant role during fruit set and the early stages of fruit development. Additionally, the high activity of gibberellin, cytokinin, and sucrose-metabolizing enzymes in the ovary was conducive to early fruit development. Furthermore, we generated high-resolution spatiotemporal gene expression profiles in the ovary from the stage of efflorescence to early fruit development. Comparative transcriptomics and weighted gene co-expression network analysis revealed specific genes and gene modules predominant at distinct developmental stages, thereby highlighting unique genetic programming. Overall, we identified the potential regulatory network governing fruit initiation and subsequent development, as well as the sets of candidate genes involved, based on the aforementioned results.

Conclusions The results offer a valuable reference and resource for the application of exogenous substances, such as hormones and sugars, during critical fruit development periods, and for the development of molecular tools aimed at improving yield.

Keywords *G. Sinensis*, Transcriptome analysis, Plant hormones, Eegulatory network

*Correspondence:
Xiurong Wang
xrwang@gzu.edu.cn
[1]College of forestry, Guizhou University, Guiyang550025, Guizhou, China
[2]Institute for Forest Resources & Environment of Guizhou, Guizhou University, Guiyang, Guizhou, China
[3]Key Laboratory of Forest Cultivation in Plant Mountainous of Guizhou Province, Guiyang, Guizhou, China
[4]Key Laboratory of Plant Resource Conservation and Germplasm Innovation in Mountainous Region (Ministry of Education), Guizhou University, Guiyang, Guizhou, China

Background

Gleditsia sinensis, a deciduous tree belonging to the genus Gleditsia in the Leguminosae family, is a unique species widely distributed in China [1, 2]. Additionally, it serves as an ecologically and economically multipurpose tree with significant development potential. Its thorns are used in traditional medicine [3–5], its wood is utilized in building materials [6], it acts as a pioneer species in ecological restoration [7], and its seeds are considered a strategic raw resource and high-grade health products [8, 9]. The majority of valuable specialized metabolites, such as triterpenoid saponins, caspicaosides, and galactomannan, are extracted from the thorn and fruit of *G. sinensis* [5, 10, 11]. Consequently, the economic forest planting area of *G. sinensis* has been continuously expanded through its introduction to various regions, particularly in southwest China, with Guizhou as a representative area [12]. Field investigations have revealed that large areas of low-yielding economic forests, characterized by low fruit set and unstable yield, not only result in a significant waste of resources but also impede the development and promotion of this industry [13]. Therefore, it is urgent to conduct research on how to improve the fruit set of economic forest in *G. sinensis* so as to achieve the purpose of increasing production and generating income.

Severe flower and fruit abscission represents a primary factor influencing fruit yield [14]. In sexually reproducing plants, double fertilization is critical for successful fruit development [15]. Successful fertilization triggers the ovary to resume growth, a process termed "fruit set" or "fruit initiation," while unfertilized flowers are typically abscised [16]. This mechanism is a result of intricate programming within the plant to ensure the successful completion of fruit development [17]. Fertilization-dependent fruit set and subsequent development are attributed to a complex regulatory network involving phytohormones, carbohydrates, related regulatory genes, and other metabolites induced by fertilization [18–24]. Consequently, the roles of plant hormones, particularly auxin and gibberellin (GA), are widely recognized in the regulation of fruit set initiation, functioning as positive regulatory signals that trigger rapid ovary growth [25–27]. Consistent with these findings, previous studies have demonstrated the feasibility of using plant growth regulators to reduce abscission and enhance fruit set [28–31]. These studies significantly enhance our understanding of the mechanisms by which plant growth regulators influence fruit set. While the general role of these hormones in the regulation of fruit setting and development has been established, the specific regulatory mechanisms can vary substantially across different plant species. It is well recognized that the efficacy of plant growth regulator applications is contingent upon various factors, including plant species, timing of application, method of application, concentration, and other variables [31–33]. Furthermore, the underlying regulatory mechanisms also differ among plant species [34–37]. A comprehensive understanding of the regulatory mechanisms governing fruit set and the dynamic functions of endogenous hormones is essential for providing precise guidance in the selection, combination, and judicious application of exogenous plant growth regulators in practical agricultural production. This knowledge facilitates the achievement of higher yields with reduced effort. However, to date, there have been no reports elucidating the mechanisms underlying fruit set and development in *G. sinensis*.

In this study, the early stages of fruit development in *G. sinensis* were investigated through morphological analysis and paraffin sectioning, spanning from the flowering phase to early fruit development. Comprehensive data encompassing endogenous non-structural carbohydrates, hormonal fluctuations, the spectrum of expressed genes, and their regulatory networks during fruit set and early developmental stages were subsequently collected. The integration of spatiotemporal transcriptomic data with endogenous hormonal changes in this study elucidates early fruit developmental processes and provides insights into the dynamic molecular mechanisms underlying fruit set and development. This research also offers a valuable reference for the identification of plant growth regulators that can enhance the fruit setting rate.

Results

Morphological characteristics of ovary during early fruit development

Significant morphological changes in the ovary were observed from 0 to 10 days after anthesis (DAA) in *G. sinensis*, particularly in terms of ovary length (Fig. 1A). Additionally, the length, width, and thickness of the ovary all exhibited an increase as the days after anthesis progressed (Fig. 1B). Among these dimensions, ovary length showed the most pronounced increase, with statistically significant differences observed between each time point. In contrast, ovary width began to increase rapidly starting at 6 DAA, with minimal changes observed between 0 and 2 DAA, as well as between 4 and 6 DAA. In comparison to the length and width of the ovary, the thickness of the ovary exhibited the least variation across different time points. Specifically, there was minimal increase in thickness from 0 days after anthesis (DAA) to 6 DAA, with a significant rise observed at 8 DAA. Concurrently, changes were noted in the stigma color and the morphology of stigma cells. The shape of stigma mastoid cells transitioned from cylindrical to withered and dehydrated, accompanied by a color change from transparent to reddish-brown (Fig. 1C). These alterations can be attributed to the recognition process between the stigma and pollen grains, as well as the subsequent hydration, germination,

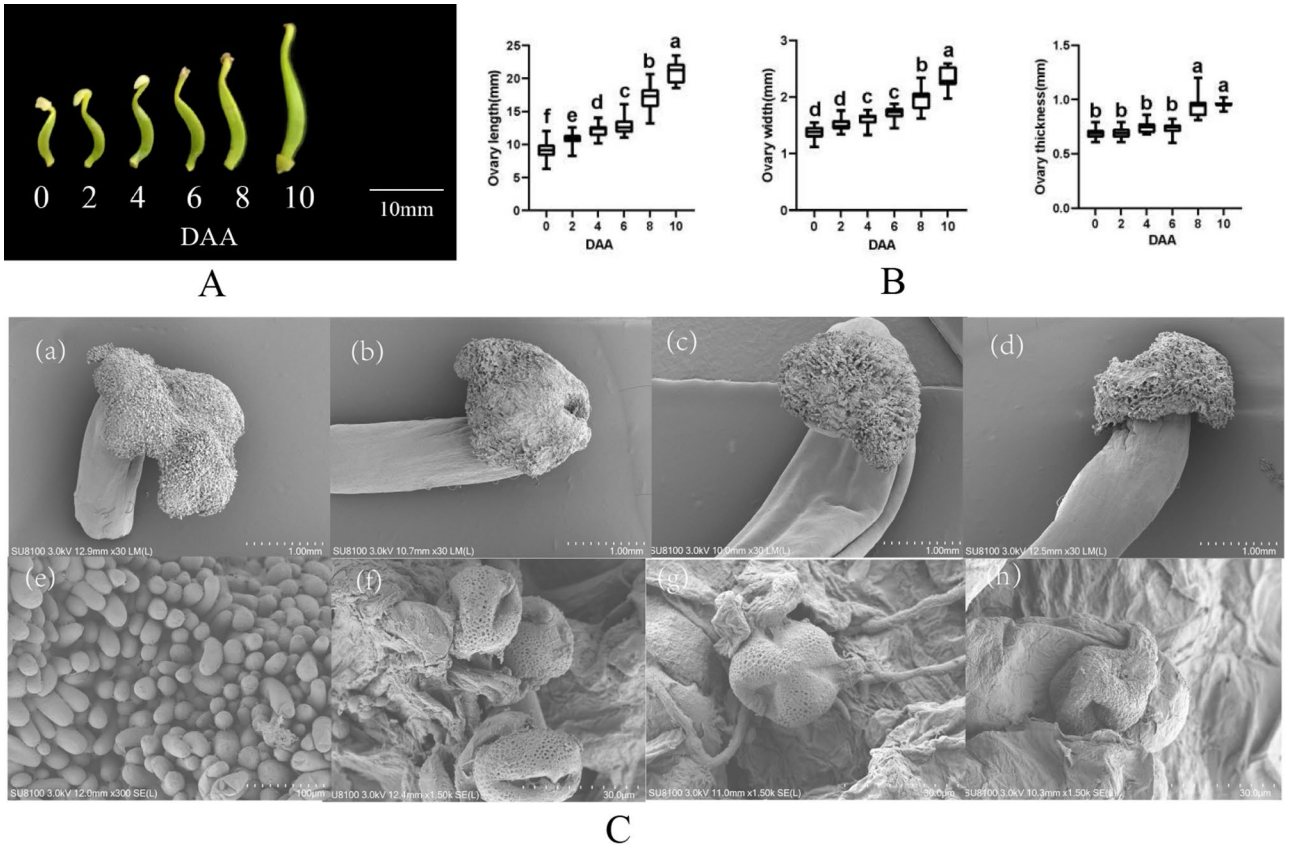

Fig. 1 An analysis of the initial stages of fruit development. **A**. Morphological changes in the ovary at six time points (Note: the numbers below the image indicate the number of days after flowering). **B**. Quantitative trait variations in the length, width, and thickness of the ovary (Note: the sample size for each time point was 30, and the ovary quantitative traits at different time points were analyzed and compared using ANOVA; vertical bars represent ± SE, and different letters indicate a significant difference at the 0.05 level). **C**. Stigma morphology at 0 DAA, 2 DAA, 4 DAA, and 6 DAA (a-d), scale bar = 1 mm; hydration and germination of pollen grains on the stigma (e-f), scale bar = 30 μm

and elongation of pollen grains on the stigma (Fig. 1C, f-h).

Fruit initiation and development are intricately linked to pollination and fertilization. To elucidate the process of fruit initiation and development, observations of pollen tube dynamics were conducted (Fig. 2). The study revealed that, 12 h post-pollination, a significant number of germinated pollen grains were present on the stigma, beginning their extension through the style canal towards the ovary. By 24 h post-pollination, a substantial number of pollen tubes had traversed the style canal and reached the upper ovules within the ovary. However, only a few pollen tubes managed to reach the ovules located at the base of the ovary at 48 h after pollination. Based on the aforementioned results, we hypothesize that the fertilization process in *G. sinensis* requires a minimum of 48 h post-pollination to reach completion. Consequently, the critical period for pollination spans from 0 days after anthesis (DAA) to 2 DAA. During this interval, the ovary appears to be in a state of arrested development, presumably in preparation for double fertilization. This hypothesis is corroborated by the observed minimal morphological changes in the ovary between 0 DAA and 2 DAA.

Observation of the microstructure of the ovary wall during early fruit development

In angiosperms, successful fertilization of the ovule initiates a series of cell divisions and expansions that culminate in fruit growth [38]. To precisely characterize the early stages of fruit development, the number of cell layers and cell sizes in cross-sections of the ovary were examined at six distinct time points (Fig. 3). Microscopic analysis revealed a significant increase in the number of endocarp cell layers at 4 days after anthesis (DAA) compared to 0 DAA and 2 DAA.Thus, the observed increase in cell layers and size of the ovaries at 6 days after anthesis (DAA) may indicate the completion of double fertilization, which subsequently initiates cell division and cell expansion within the ovary.

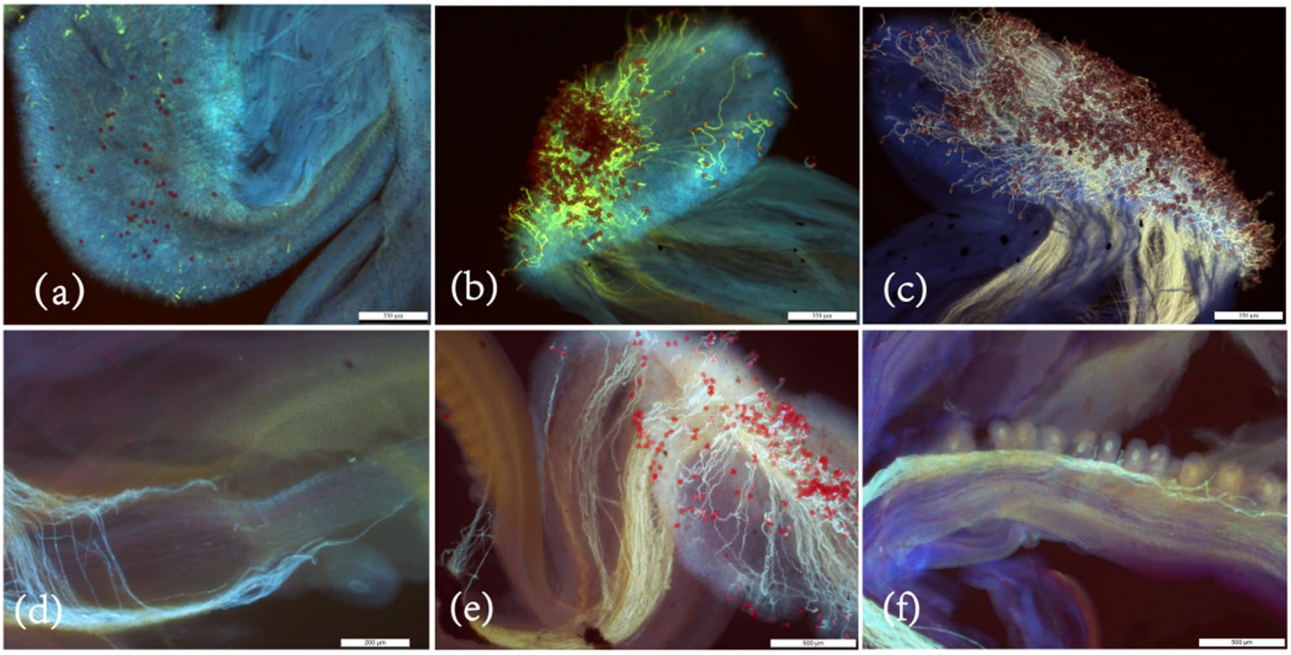

Fig. 2 Pollen tube growth dynamics after pollination. **a**,1 h after pollination; **b**, 3 h after pollination; **c**, 12 h after pollination; **d**, 24 h after pollination; **e**, 36 h after pollination; **f**, 48 h after pollination; scale bar = 350 μm(**a**-**c**), 200 μm(**d**), 500 μm(**e**-**f**)

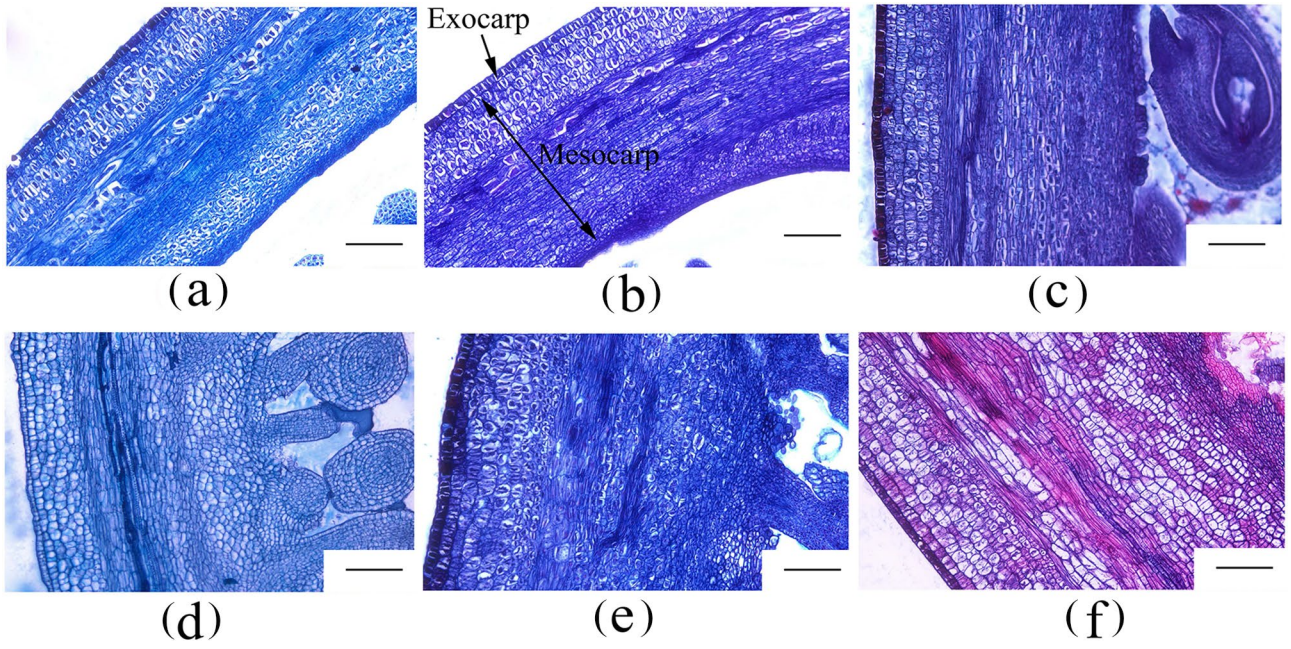

Fig. 3 Cell morphology observation of the ovary wall during early fruit development. **a**-**f**, cell morphology of ovary wall on 0, 2, 4, 6, 8 and 10 DAA. DAA, days after anthesis; Ex, Exocarp; Me, Mesocarp; Scale bar = 200 μm

Observation on the microstructure of embryo sac in ovule during early fruit development

Given that successful fertilization stimulates the ovary to transition from a dormant state to active growth, we further examined the changes in the two polar nuclei and the egg cell within the embryo sac during the early stages of fruit development in *G. sinensis* (Fig. 4). Observations indicated that on 0 DAA (days after anthesis), the two polar nuclei situated in the center of the embryo sac and the egg nucleus near the micropyle were distinctly visible (Fig. 4a). Subsequently, the two polar nuclei fused into one, preparing for fertilization along with the egg cell. By 2 DAA, two released spermatosomes were observed moving towards the polar nuclei and the egg cell (Fig. 4b).

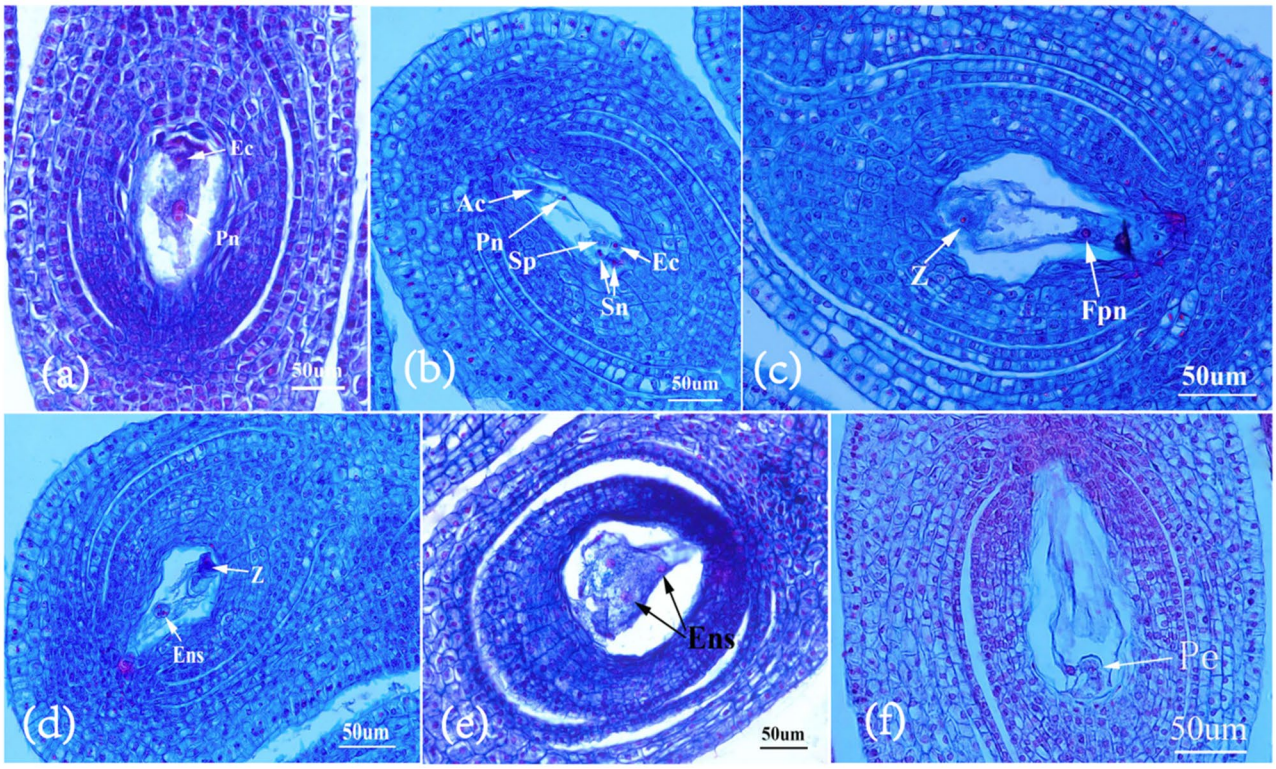

Fig. 4 Changes in embryo sac after different anthesis during early fruit development in *G. sinensis*.**a**,Mature embryo sac on 0 DAA; **b**, Two polar nuclei fuse into one and two sperm nuclei were moving to the egg and polar nucleus on 2 DAA; **c**, An egg cell and a polar nucleus that have undergone double fertilization on 4 DAA; **d**, The fertilized polar nuclei begin to fission on 6 DAA; **e**, Endosperm cells has undergone division on 8 DAA; f, Multicellular proembryo on 10 DAA. AG, Antipodal Group; Sn, Synergid; EC, Egg Cell; Sp, Sperm nucleus; Fpn, Fertilized polar nuclei; Z, Zygote; Ens, Endosperm; Pe, proembryo; Scale bar = 50 μm

Following double fertilization, the fertilized egg and polar nuclei were distinctly visible within the embryo sac at 4 days after anthesis (DAA) (Fig. 4c). Subsequently, the fertilized polar nuclei commenced nuclear division between 6 DAA and 8 DAA (Fig. 4d-f). Ultimately, a zygote with a multicellular proembryo was formed after several cell divisions, which was clearly observed in the embryo sac at 10 DAA (Fig. 4f). This microscopic progression was consistent with the external manifestations of early fruit development, suggesting that the critical period for fertilization occurred between 2 DAA and 4 DAA, with the initiation of fruit development beginning at approximately 6 DAA.

Changes in non-structural carbohydrates dynamics during early fruit development

Considering that carbohydrate metabolism has been documented to play a role in early fruit development [21, 23], we investigated the content of non-structural carbohydrates, including sucrose, glucose, fructose, soluble sugars, and starch, in ovaries at six distinct time points to elucidate their roles in early fruit development (Fig. 5). The levels of sucrose and fructose in the ovary significantly decreased following pollination and remained relatively low during the stages of fertilization and subsequent fruit development. The glucose content in the ovary exhibited a slight increase during pollination and fertilization, subsequently peaking at 6 days after anthesis (DAA) and remaining stable thereafter. In contrast, the soluble sugar content in the ovary remained relatively stable, with the exception of a significant decline observed at 8 DAA. The levels of fructose and sucrose demonstrated an inverse trend compared to glucose. These findings suggest that the elevated glucose content may be associated with the decomposition of sucrose and the conversion of fructose during the early stages of fruit development. The starch content in the ovary exhibited irregular fluctuations, peaking at 2 days after anthesis (DAA) and reaching its lowest levels at 4 DAA and 8 DAA. These findings suggest that the concentrations of sucrose, glucose, fructose, soluble sugars, and starch in the ovary undergo significant temporal variations, potentially linked to their roles in early fruit development.

Activities of sucrose synthase (SSI, SSII), invertase (AI, NI) in ovaries of *G. sinensis* during early fruit development stage

The activities of sucrose synthase and invertase in the ovary were also measured to investigate their roles in

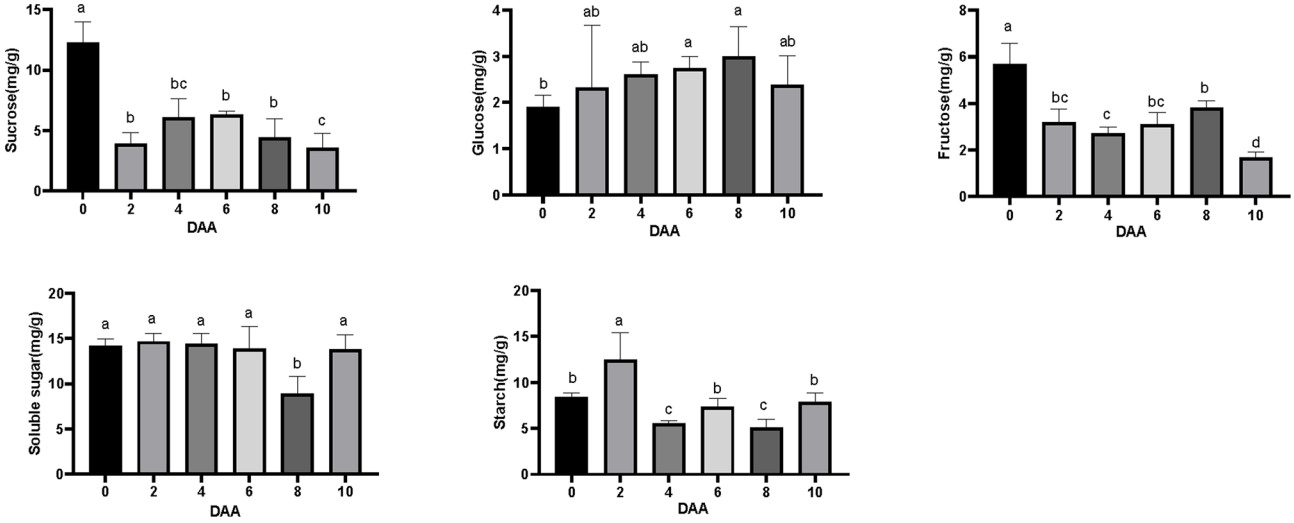

Fig. 5 Content of sucrose, glucose, fructose, soluble sugar and starch in ovary of *G. sinensis* during the early fruit development stage.Vertical bars represent ± SE, different letters show a significant difference at the 0.05 level

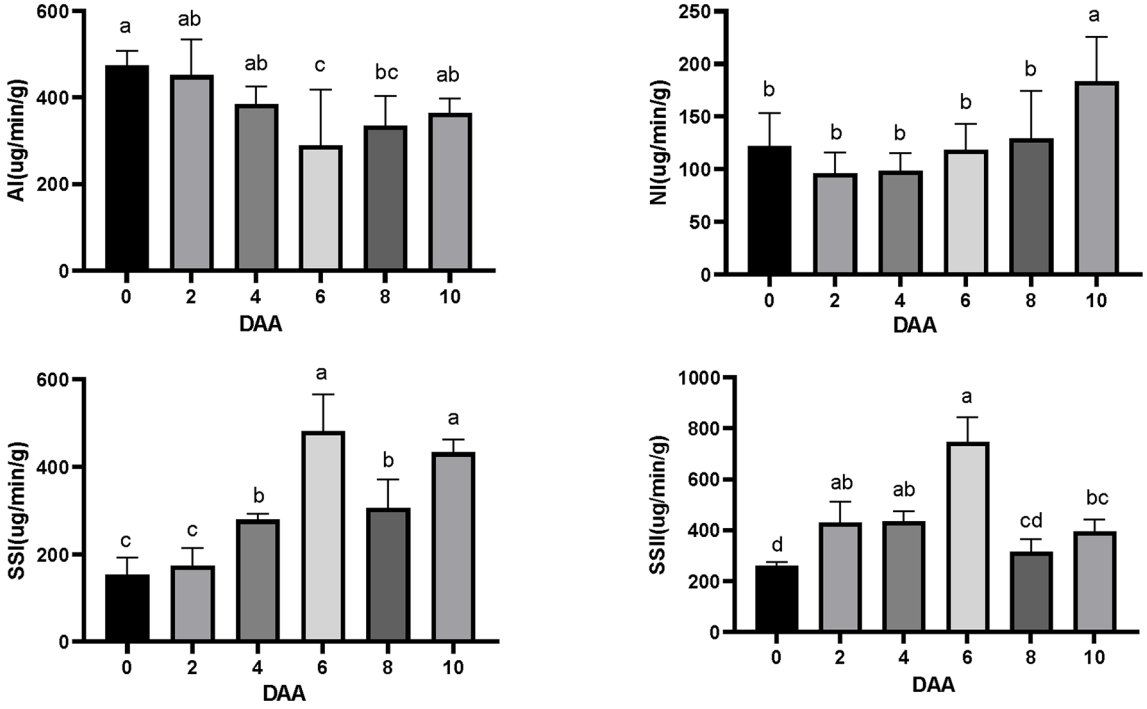

Fig. 6 Activities of ovary sucrose synthase (SSI, SSII) and invertase (AI, NI) in *G. sinensis* during the early fruit development stage. DAA, days after anthesis. Vertical bars represent ± SE, different letters show a significant difference at the 0.05 level

fruit set and development [39–41]. The acid invertase (AI) activity in the ovaries exhibited an initial decline followed by an increase, ultimately reaching its lowest level at 6 days after anthesis (DAA) (Fig. 6a). In contrast, the neutral invertase (NI) activity in the ovary remained relatively stable from 0 to 8 DAA, with a significant increase observed at 10 DAA (Fig. 6b). The activities of SSI (Sucrose Synthase I) and SSII (Sucrose Synthase II) in the ovary significantly increased from 0 days after anthesis (DAA) to 6 DAA, reaching their peak at 6 DAA, and subsequently decreased significantly by 8 DAA (Fig. 6c-d). These variations indicate that sucrose synthase and invertase function at distinct times during the early stages of fruit development. When considered in conjunction with the early fruit development process, these findings suggest that sucrose synthase is crucial during pollination and fertilization, whereas sucrose invertase is associated with ovary development post-fertilization.

Changes in hormonal dynamics during early fruit development

Auxin and cytokinin

To further elucidate the role of hormones in early fruit development in *G. sinensis*, we analyzed hormone content using HPLC-MS/MS (Fig. 7). The results indicated the presence of three auxin-related compounds: Indole-3-acetic acid (IAA) and its two amide conjugates, indole-3-acetylaspartic acid (IAAsp) and indole-acetylalanine (IAAla). Despite variations in their forms and quantities, all three compounds exhibited a similar trend, with a gradual increase following pollination, peaking at 6 days after anthesis (DAA), and subsequently declining. However, the amount of IAA did not differ significantly among the six time points examined. Given that IAAsp is a catabolite of IAA [42], and IAAla contributes to maintaining auxin dynamic balance, it suggests that auxin dynamics, rather than auxin levels triggered by pollination and fertilization, play a crucial role in the early fruit development of *G. sinensis*. Regarding cytokinin, the amount of tZR increased rapidly from 6 days after anthesis (DAA), likely associated with the rapid division of the endosperm following fertilization.

Gibberellin

It is well established that gibberellin is among the most potent hormones influencing fruit set and development [23]. In this study, seven types of gibberellins, specifically GA1, GA3, GA4, GA7, GA8, GA9, and GA24, were identified in the ovaries of *G. sinensis* during the early stages of fruit development. According to previous research, only GA1, GA3, GA4, and GA7 exhibit biological activity, whereas GA8 is an inactive product resulting from GA1 catabolism, and GA9 and GA24 serve as precursors to GA4 [43, 44]. Although the levels of GA3, GA4, and GA7 all exhibited an increasing trend during ovary development, only GA7 showed a significant increase upon fertilization at 4 days after anthesis (DAA), suggesting its crucial role in the fertilization process. In contrast, the levels of GA3 and GA4 increased rapidly starting at 6

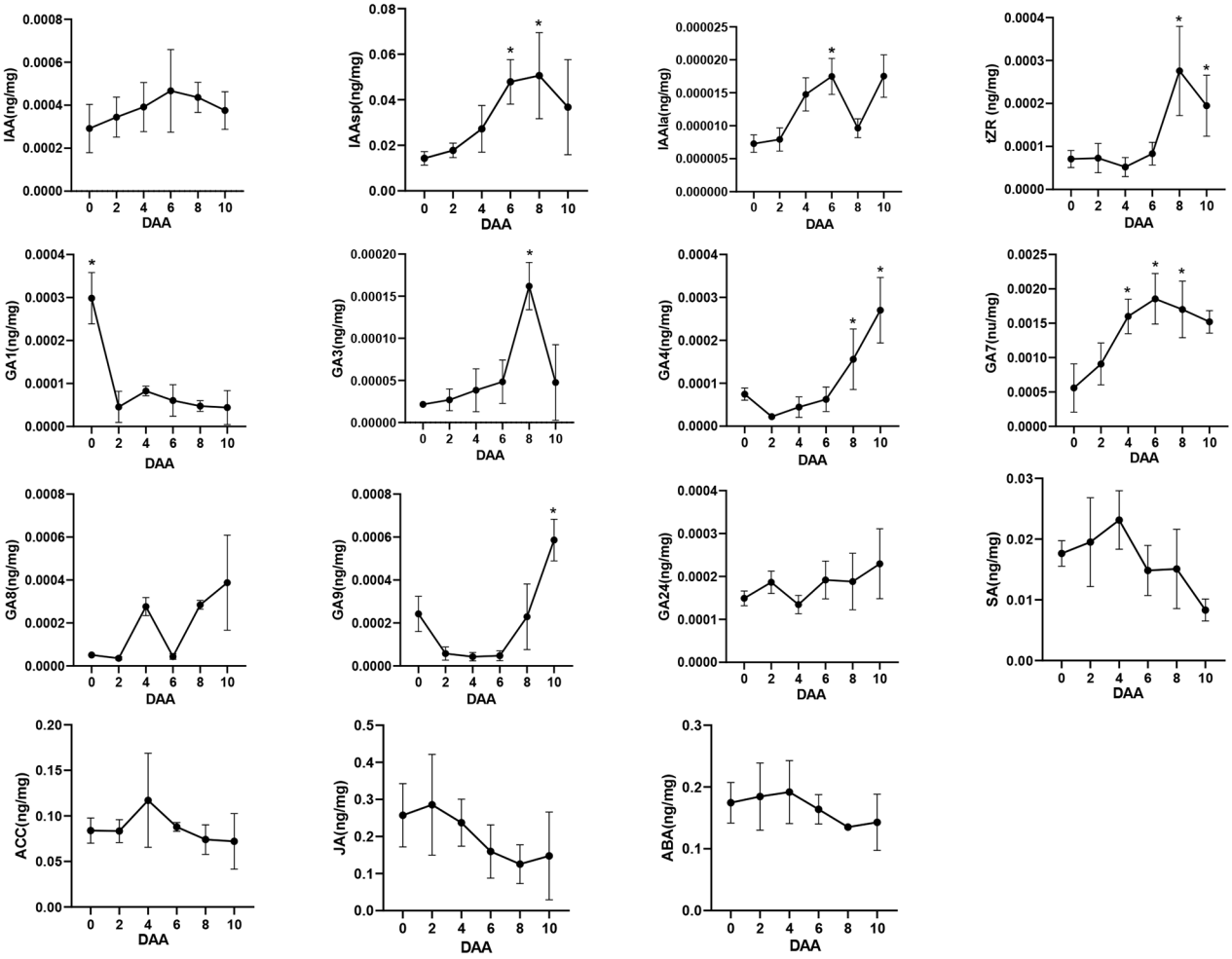

Fig. 7 Hormonal dynamics of ovaries in *G. sinensis* during early fruit development stage. DAA, days after anthesis.Vertical bars represent ± SE. Significant difference at 5% level is indicated by *

DAA, indicating their primary involvement in early fruit development post-fertilization. Unlike these three bioactive gibberellins, the level of GA1 decreased significantly following pollination and remained consistently low thereafter. Furthermore, the elevated levels of GA8 and GA9, as an inactive catabolite and a precursor respectively, corresponded with the observed decrease and increase in the levels of GA1 and GA4. These findings collectively suggest that the synthesis and metabolism of gibberellins are intricately associated with the early fruit development of *G. sinensis*.

SA, JA, ACC and ABA

Our study revealed that salicylic acid (SA), jasmonic acid (JA), abscisic acid (ABA), and 1-aminocyclopropane carboxylic acid (ACC), a precursor in ethylene synthesis, were detected during the early fruit development of *G. sinensis*. Notably, the concentrations of SA and ACC exhibited a similar pattern, initially increasing from 0 days after anthesis (DAA) to 4 DAA, and subsequently decreasing after reaching their peak at 4 DAA. In contrast, the levels of JA and ABA in the ovaries remained relatively stable initially, but began to decline progressively from 4 DAA onwards.

Correlation analysis between physiological indexes of ovary and ovary growth traits during early fruit development

To gain a deeper understanding of the relationship between ovary growth morphology and various indices, a correlation analysis was performed (Fig. 8). The findings revealed that ovary morphological traits exhibited significant negative correlations with fructose, soluble sugar, AI activity of the ovary, and JA, while showing positive correlations with NI, SSI, GA4, GA9, and tZR. These results suggest that elevated activities of gibberellin, cytokinin, and sucrose-metabolizing enzymes in the ovary are conducive to early fruit development.

Transcriptome profile of *G. sinensis* early fruit development

To elucidate the dynamic transcriptome profiles during early fruit development and to uncover the molecular mechanisms underlying this process, RNA-seq analysis was conducted on ovaries collected at various developmental stages (0, 2, 4, 6, 8, and 10 days after anthesis,

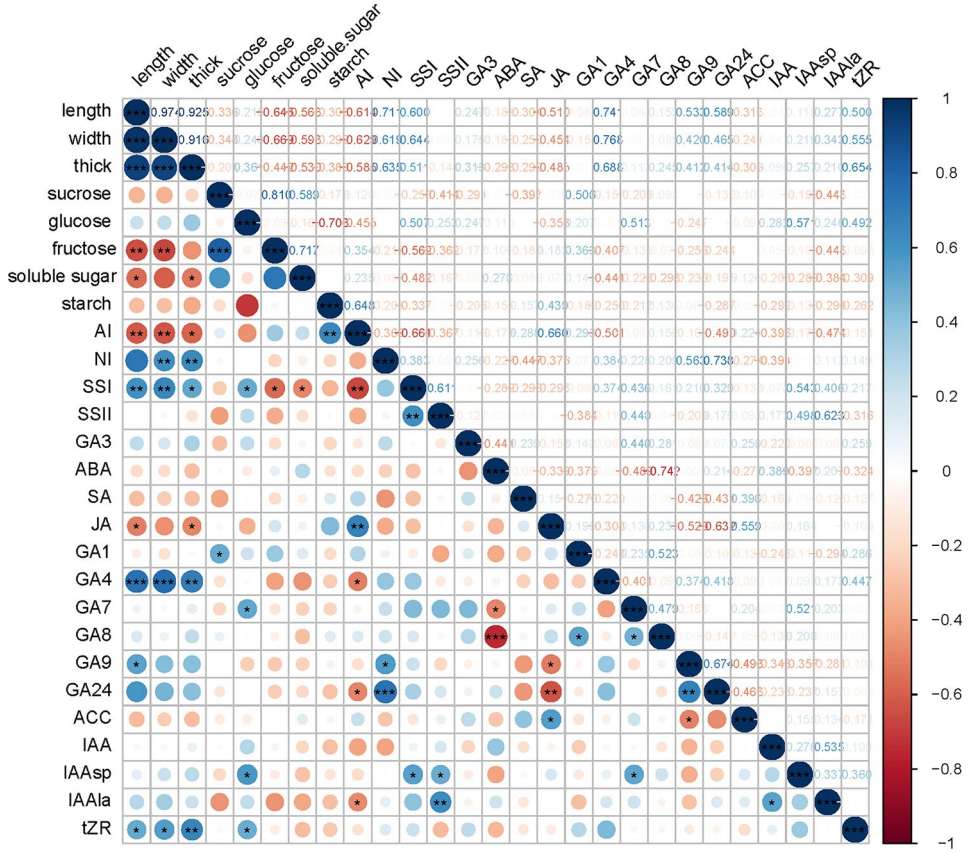

Fig. 8 Correlation heat map between ovary growth traits and physiological indexes of *G. sinensis* during early fruit development. * means that the correlation is significant at the significance level of 0.05, **means that the correlation is significant at the significance level of 0.01, and *** means that the correlation is significant at the significance level of 0.001

denoted as D0, D2, D4, D6, D8, and D10, respectively). Three biological replicates were utilized to construct the corresponding RNA-seq libraries. The number of trimmed sequencing reads ranged from 43,541,126 to 66,313,258, with the percentage of uniquely mapped reads varying between 80.13% and 81.91% for each sample (Supplementary Table S1). Following the quantitative analysis of gene and transcript expression levels using the RSEM software (Supplementary Table S2), a Venn diagram and correlation analysis among samples were conducted based on the expression matrix (Fig. 9A and S1). A total of 23,749 unigenes were found to be shared across all time points when the gene expression threshold was set at 1. The specific expression genes for D0, D2, D4, D6, D8, and D10 were 3,146, 2,232, 2,494, 2,095, 1,566, and 2,609, respectively. Only transcripts exhibiting a significant (FDR < 0.05) two-fold difference in expression between any two samples were considered as differentially expressed genes (DEGs) (Supplementary Table S3).The number of differentially expressed genes (DEGs) between the two groups, as reported in Supplementary Table S2, is summarized in Supplementary Table S4. The number of DEGs between two consecutive time points was relatively lower (Fig. 9B). Specifically, the group with the fewest DEGs was D6 vs. D4, while the group with the greatest number of DEGs was D8 vs. D6. Notably, the highest number of DEGs was observed between D10 and D4 across all groups. These findings suggest that D4 and D6 may represent critical transition time points, serving as key nodes in the transition between fertilization and fruit development, which aligns with the changes of related physiological indexes and hormones.

To elucidate the role of differentially expressed genes (DEGs) during early fruit development, Gene Ontology (GO) enrichment analysis was conducted on DEGs across various time points, with the top five GO terms for each group presented in Fig. 9C. The analysis revealed the involvement of multiple molecular functions and metabolic processes in early fruit development. Notably, several GO terms, including "DNA replication initiation," "double-strand break repair via break-induced replication," "cytoplasmic translation," "pectin catabolic

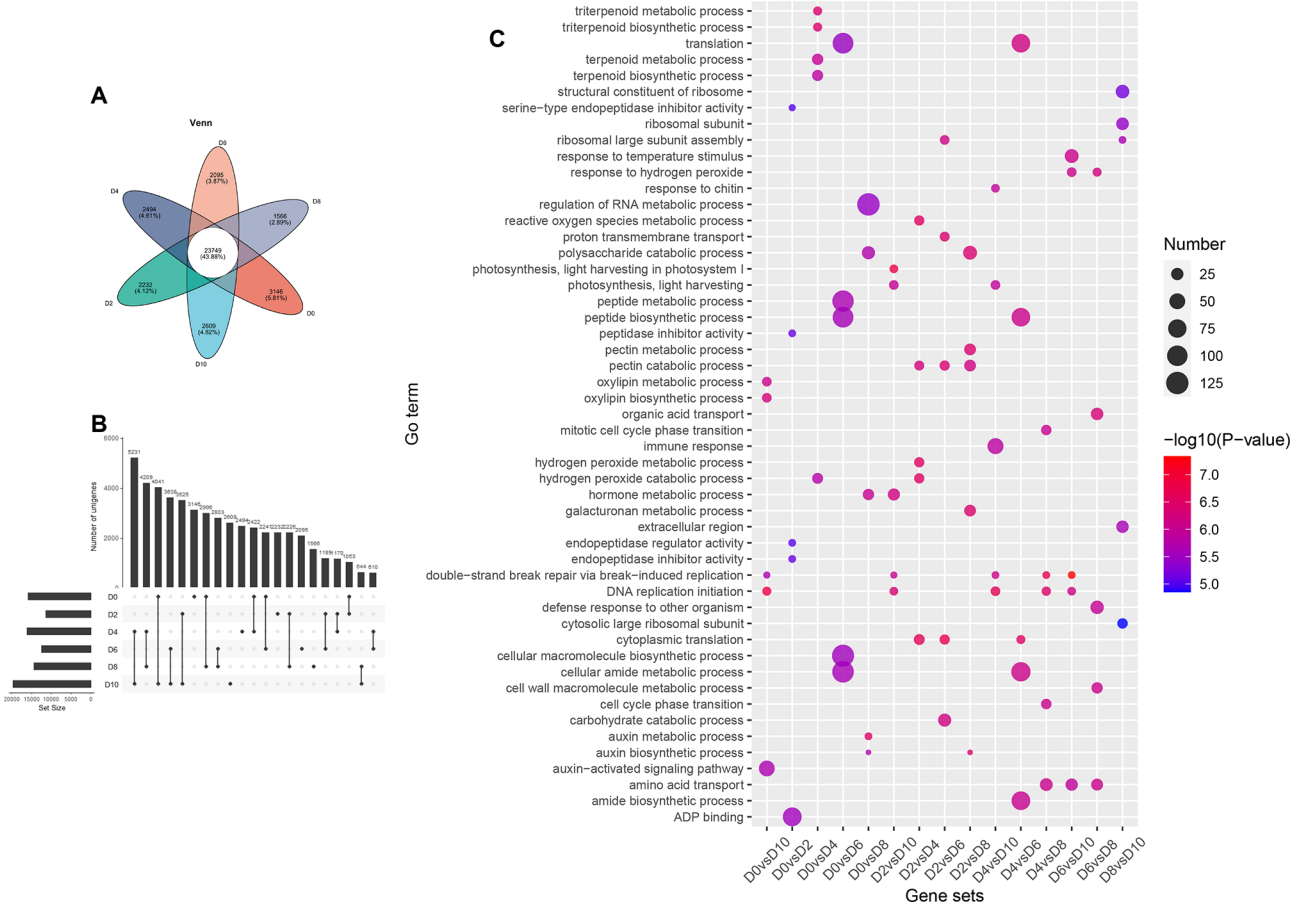

Fig. 9 Analysis of DEGs during early fruit development. **A**, Venn petal map between samples, the number of genes common to all samples (central region) and the number of genes specific to each sample (petal regions). **B**, UpSet plot showing the number of DEGs between two time points during early fruit development. The DEGs number is shown by the bar and number above the dot. Individual dots show the number of genes specifically expressed in that sample. **C**, GO enrichment analysis of DEGs in different gene sets

process," "amino acid transport," and "hormone metabolic process," were common across different groups. However, certain functional categorizations of differentially expressed genes (DEGs) were exclusively enriched in specific groups. For instance, terpenoid metabolic and biosynthetic processes were solely identified in the D0vsD4 group, while the auxin metabolic process was enriched only in the D0vsD8 group. Additionally, endopeptidase regulator and inhibitor activity, as well as oxylipin biosynthetic and metabolic processes, were observed exclusively in the D0vsD2 and D0vsD10 groups, respectively. Our transcriptomic analysis revealed that some genes remained active throughout the early stages of fruit development, whereas the expression of other genes was induced and became prominent at distinct developmental time points.

Time-course RNA-seq analysis during early fruit development

We conducted an analysis of variance (ANOVA)-like test to identify differentially expressed genes (DEGs) across six time points, resulting in the identification of 10,898 unigenes exhibiting dynamic expression patterns during the early fruit development of *G. sinensis*. To categorize genes with similar expression profiles, we employed the K-means clustering algorithm, which grouped the genes based on the similarity of their transcriptomic profiles (Fig. 10). Consequently, six distinct clusters were identified. Additionally, Gene Ontology (GO) enrichment analysis was performed for each cluster to elucidate the functional roles of the genes within these clusters. In Cluster 1 (C1), 1785 genes exhibited a general downward trend from day 0 (D0) to day 10 (D10), with the most rapid downregulation occurring between D0 and D2, followed by a stable decline. Functional categorization of the differentially expressed genes (DEGs) in C1 indicated that genes associated with "ovary arrest" downregulated by pollination are linked to categories such as "nutrient reservoir activity," "terpene synthase activity," "ribonuclease T2 activity," "protein-N-terminal asparagine amidohydrolase activity," and "acid-amino acid ligase activity." A total of 1,703 genes exhibited analogous

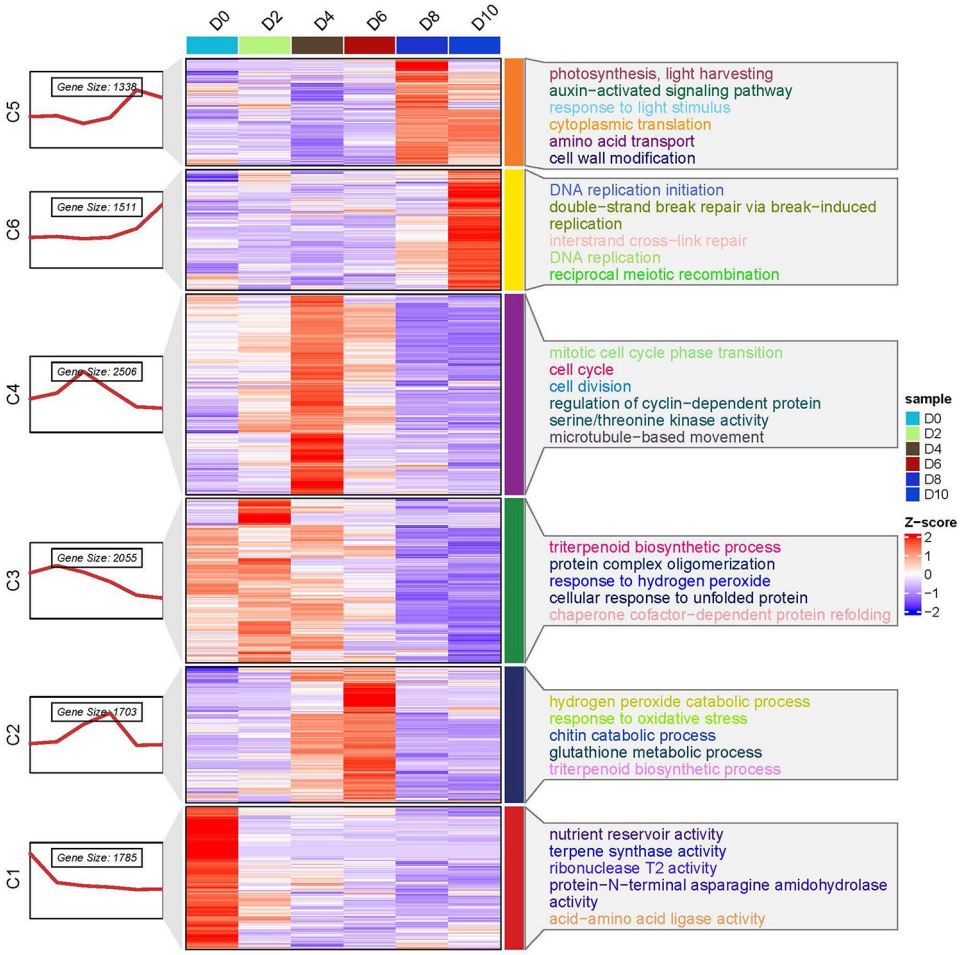

Fig. 10 Analysis of gene expression patterns in time series (DEGs) during early fruit setting. a K-means clustering analysis of the DEGs into six clusters according to their expression profile. The cluster names and the number of unigenes for each cluster are indicated

expression patterns within Cluster 2 (C2), characterized by a progressive up-regulation from day 2 (D2) to day 6 (D6), followed by a gradual down-regulation post-peak at D6. This cluster was notably enriched with gene categories associated with "hydrogen peroxide catabolic process," "response to oxidative stress," "chitin catabolic process," "glutathione metabolic process," and "triterpenoid biosynthetic process." Considering these results in conjunction with the findings from morphological identification, we propose that the activation of genes related to oxidative stress and antioxidant defense during the double fertilization of **G. sinensis** may be attributable to the role of reactive oxygen species (ROS) in pollination and fertilization [51]. Specifically, 2055 genes exhibited a gradual up-regulation from day 0 (D0) to day 2 (D2), followed by a gradual down-regulation post the D2 peak within Cluster 3 (C3). Gene Ontology (GO) terms such as "triterpenoid biosynthetic process," "protein complex oligomerization," "response to hydrogen peroxide," "cellular response to unfolded protein," and "chaperone cofactor-dependent protein refolding" were enriched in this cluster. This enrichment suggests that these processes, induced by pollination, may be associated with the interaction between pollen and stigma [52, 53]. In Cluster 4 (C4), 2,506 differentially expressed genes (DEGs) exhibited similar expression patterns, characterized by a gradual up-regulation from day 0 (D0) to day 4 (D4), followed by a gradual down-regulation after the peak at D4. Several Gene Ontology (GO) terms associated with cell division, including "mitotic cell cycle phase transition," "cell cycle," "cell division," "regulation of cyclin-dependent protein serine/threonine kinase activity," and "microtubule-based movement," were found to be enriched. This enrichment correlates with the observed increase in the number of endocarp cell layers at 4 days after anthesis (4DAA). A total of 1,388 genes exhibited a similar expression pattern within Cluster 5 (C5). The expression levels of these genes progressively increased from day 0 (D0) to day 8 (D8), followed by a gradual decrease after reaching the peak at D8. Functional categorization of these genes indicated significant enrichment in categories associated with "photosynthesis," "light harvesting," "auxin-activated signaling pathway," "response to light stimulus," "cytoplasmic translation," and "amino acid transport." In Cluster 6 (C6), 1511 genes exhibited minimal variation from D0 to D6, followed by a marked up-regulation commencing at D6 and peaking at D10. The findings suggest that the up-regulated genes associated with the initiation of fruit development are predominantly involved in processes related to cell division, including "DNA replication initiation," "double-strand break repair via break-induced replication," "interstrand cross-link repair," "DNA replication," and "reciprocal meiotic recombination." These results align with the timing of polar nucleus division and the preparation of the zygote for division, as observed through microscopic analysis. Collectively, these findings demonstrate a complex and dynamic alteration in transcriptional profiles during the early stages of fruit development in *G. sinensis*. Additionally, they reveal the expression of genes associated with distinct biological processes and molecular functions within the ovaries.

Potential transcriptional regulation mechanisms

To gain a comprehensive understanding of transcriptional regulation throughout the successive stages of early fruit development, an unbiased weighted gene co-expression network analysis (WGCNA) was conducted utilizing a scale-free topology model [54]. A total of 6,741 expressed genes were utilized for Weighted Gene Co-Expression Network Analysis (WGCNA), leading to the identification of 25 distinct modules (Fig. 11). Each module was associated with a module eigengene (ME), which served as an idealized representative gene reflecting the overall expression pattern within the module. The number of genes per module ranged from 47 (ME25) to 1,324 (ME0). Several modules exhibited significant ($P<0.05$) positive or negative correlations with fruit morphology and physiological characteristics. Specifically, two modules (MEturquoise and MEpink) demonstrated positive correlations, while two modules (MEred and MEsalmon) exhibited negative correlations with growth traits of *G. sinensis* during early fruit development. Consequently, these four modules were selected as hub-modules for this study (Fig. 12). Subsequently, KEGG enrichment analysis was conducted to elucidate the pathways associated with the four modules (Fig. 13). The analysis revealed that pathways related to phytohormones, including "Plant hormone signal transduction, "Zeatin biosynthesis," "Diterpenoid biosynthesis", "Cytochrome P450" and "Carotenoid biosynthesis" were enriched in the salmon module. Pathways related to protein synthesis and metabolism, including "Protein processing in the endoplasmic reticulum", "Oxidative phosphorylation", "Proteasome", "Ubiquitin-mediated proteolysis", "Protein export" and "Photosynthesis – antenna proteins" were enriched in the red module. Additionally, pathways associated with RNA and DNA, such as "RNA degradation", "Ribosome biogenesis in eukaryotes", "Nucleocytoplasmic transport", "Spliceosome", "DNA replication", "Nucleotide excision repair", "Mismatch repair" and "Homologous recombination" were enriched in the pink and turquoise modules, respectively. These findings indicate that plant hormones, protein synthesis, and metabolism, along with the replication and expression of associated genes, collectively play a crucial role in the early fruit setting of *G. sinensis*.

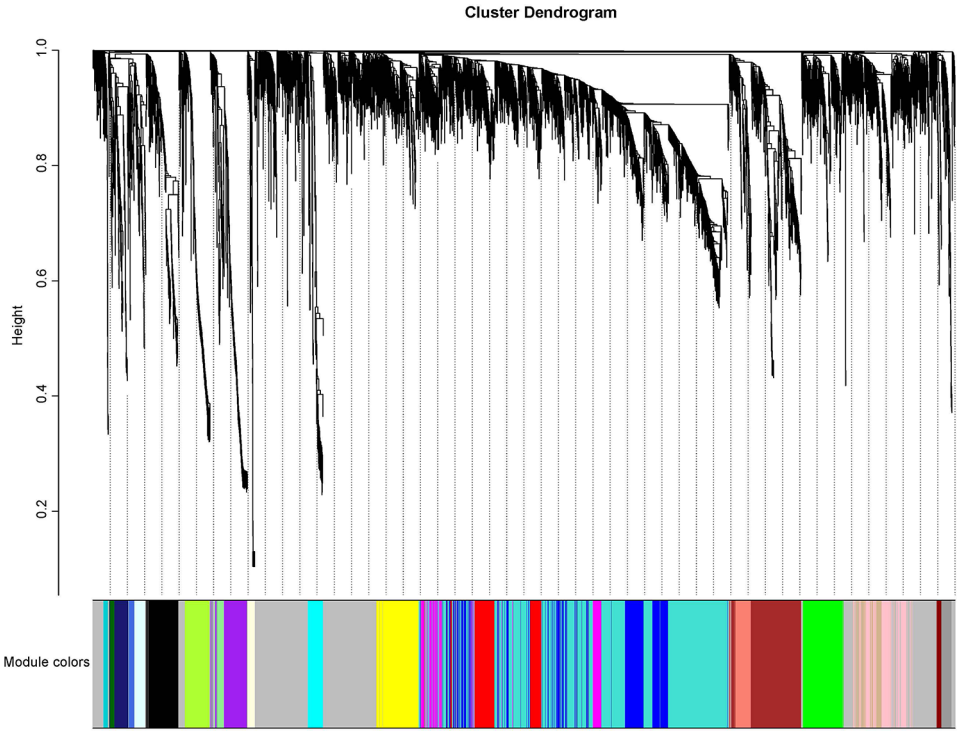

Fig. 11 Construction of the gene coexpression network during *G. sinensis* early fruit setting coloration through WGCNA. Gene dendrogram obtained by hierarchical clustering with the module color indicated by the color of the row underneath. A total of 25 distinct modules were identified

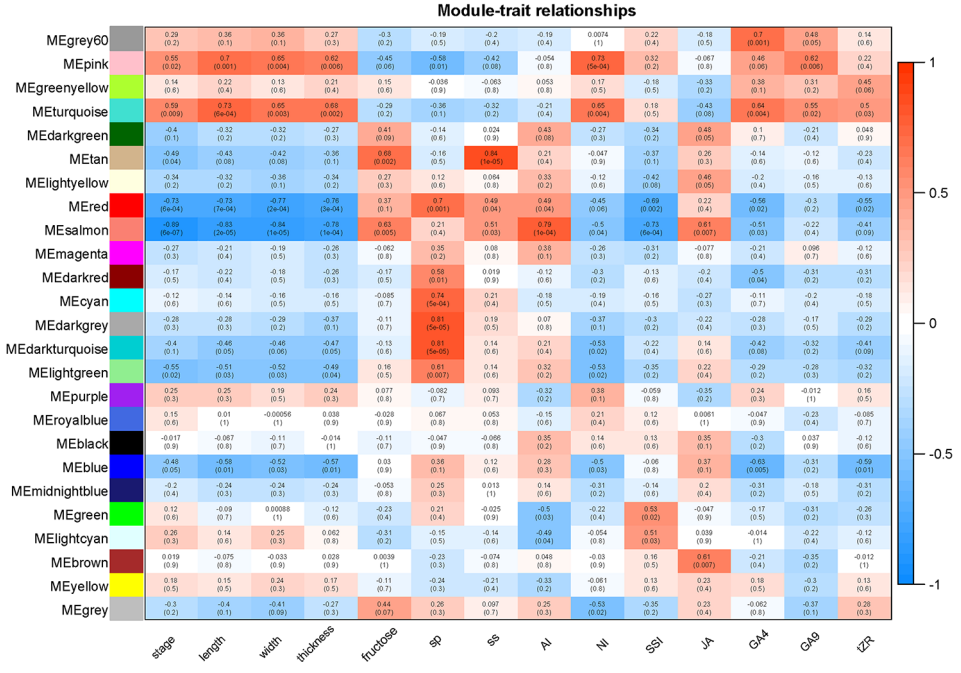

Fig. 12 Relationships of modules and different growth traits and physiological indexes. Each row in the table corresponds to a module, and each column corresponds to a growth trait

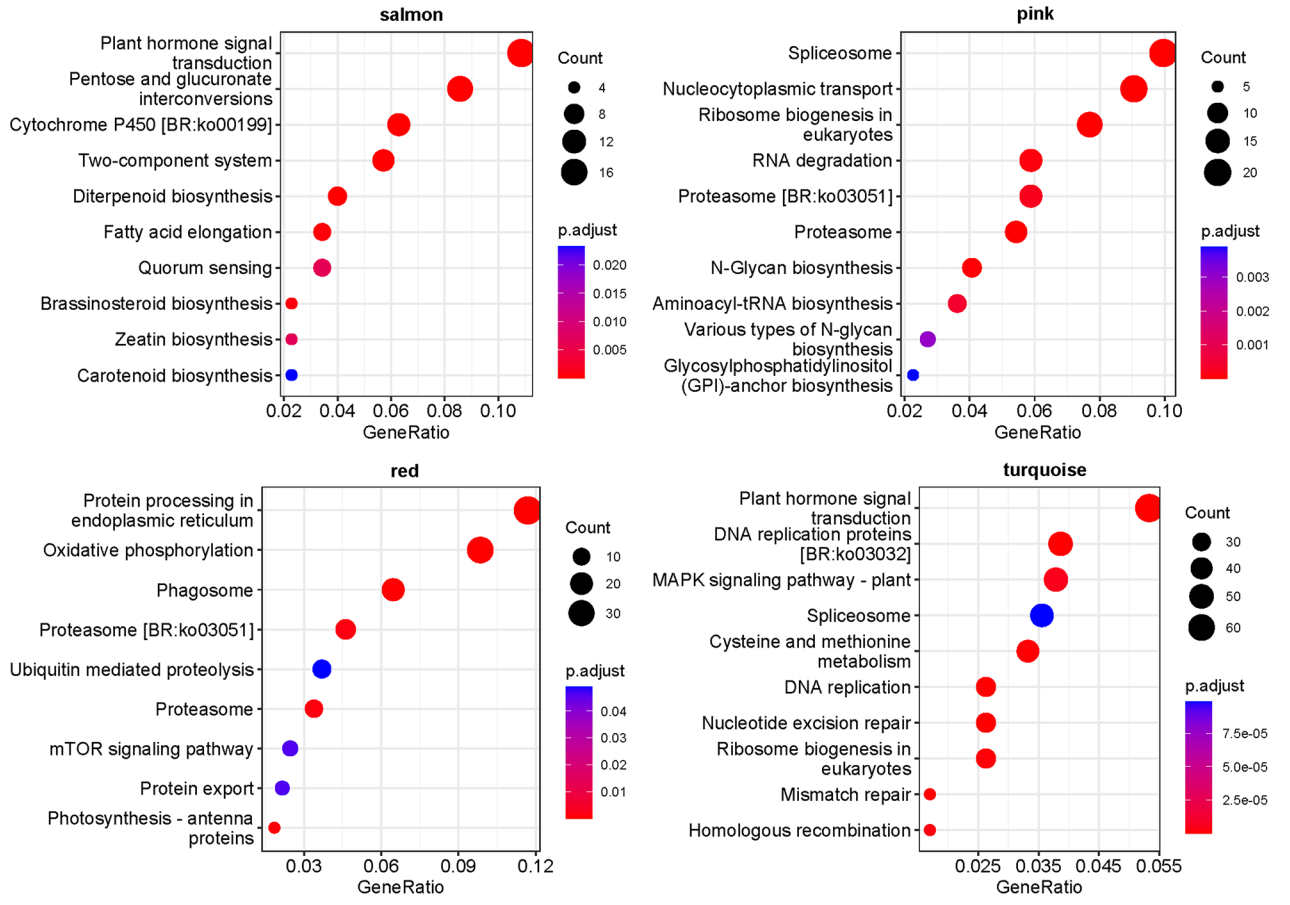

Fig. 13 Enrichment of KEGG pathway in the gene set of modules (the ordinate is the name of KEGG pathway, and the horizontal coordinate is GeneRatio, representing the ratio of the proportion of differentially expressed genes annotated to a pathway to the proportion of all expressed genes annotated to this pathway)

Hormone-related genes in ovaries of *G. sinensis* during early fruit development

Plant hormones are recognized to play a crucial role in the initiation and development of fruit [22, 23]. In this study, the biosynthesis and signal transduction pathways of plant hormones were found to be enriched in two gene modules closely associated with fruit morphology. Consequently, we identified 114 essential genes related to plant hormones that are critical for early fruit development, with 45 genes from the salmon module and 69 genes from the turquoise module (Supplementary Tables S5 and S6). The results demonstrated that several genes implicated in plant hormone biosynthesis and signal transduction pathways were predominantly expressed at a specific time point during early fruit development (Supplementary Figures S2 and S3). Notably, certain genes, such as *GA2ox*, *MAPKKK17_18*, *WRKY33*, *CYP734A1*, CCS1, *SAUR*, *ABF*, *GA3ox*, *CYP90B1*, were exclusively up-regulated at D0, indicating their collaborative role in maintaining the static state of the ovary. Additionally, several auxin-related genes, including *IAA1*, *AUX1*, *ARF*, *GH3*, together with *GA20ox*, *JAZ*, *BAK1* exhibited up-regulation from D0 to D2, followed by down-regulation post-D2. This suggests that these genes may have functional roles during pollination and pollen tube growth. Furthermore, *SAUR32* and *ETR1* were specifically up-regulated, whereas *ABF*, *IAA11*, and *IAA13* were specifically down-regulated at D4.

This study demonstrated the synergistic and antagonistic interactions among genes involved in the regulation of the same biological process. Specifically, at D6, genes such as *EBF1_2*, *SAUR10* and *PR1* were significantly up-regulated, while *NPR1* was notably down-regulated. At D8, genes including *PYL*, *BSK* and *SAUR50* exhibited high expression levels, whereas *TGA*, *ARR-B*, *PIF3* and *BAK1* were expressed at lower levels. By D10, a multitude of genes associated with auxin, gibberellin, zeatin, ethylene, abscisic acid and brassinosteroid—such as *IAA14*, *ARF5*, *SAUR50*, *AUX1*, *DELLA*, *ARR-A*, *ARR-B*, *AHP*, *ERF2*, *SNRK2*, *TGA* —were highly expressed. This indicated that the early developmental stages were

characterized by complex regulatory dynamics involving multiple hormonal pathways [55–57].

Transcriptional networks of genes during early fruit development

To elucidate the key genes and enzymes implicated in the early fruit development of *G. sinensis*, we investigated the top 30 hub genes within four distinct modules (Fig. 14). The findings revealed that a substantial number of RPS and RPL genes, which encode ribosomal proteins, emerged as core components of the regulatory network in both the turquoise and red modules. In the pink module, genes involved in cell cycle regulation, RNA splicing, and protein transport, including *DHX36*, *LARS*, and *PNPT1*, were identified as central regulatory elements. The principal genes within the regulatory network of the salmon module were implicated in plant hormone and sugar metabolism enzymes. Specifically, the genes *SAUR*, *GA3ox*, *CYP707A*, *CKX*, *ABF*, *JAR4* and *JAZ* were associated with auxin, gibberellin, cytokinin, abscisic acid and jasmonic acid respectively. This association underscores the significance and complexity of the inter-regulation of these hormones in the early stages of fruit development [44, 58–62]. Furthermore, additional genes such as *PPP2R5*, which is involved in protein phosphorylation, and *UBE2G1*, associated with protein ubiquitination, as well as genes encoding enzymes classified as E1.10.3.3, E3.2.1.67, and E3.1.1.11, were found to be co-expressed with hormones. This co-expression suggests a potential direct involvement of these genes in fruit growth. Collectively, these findings imply that early fruit development is a complex regulatory process necessitating the coordinated interaction of multiple genes.

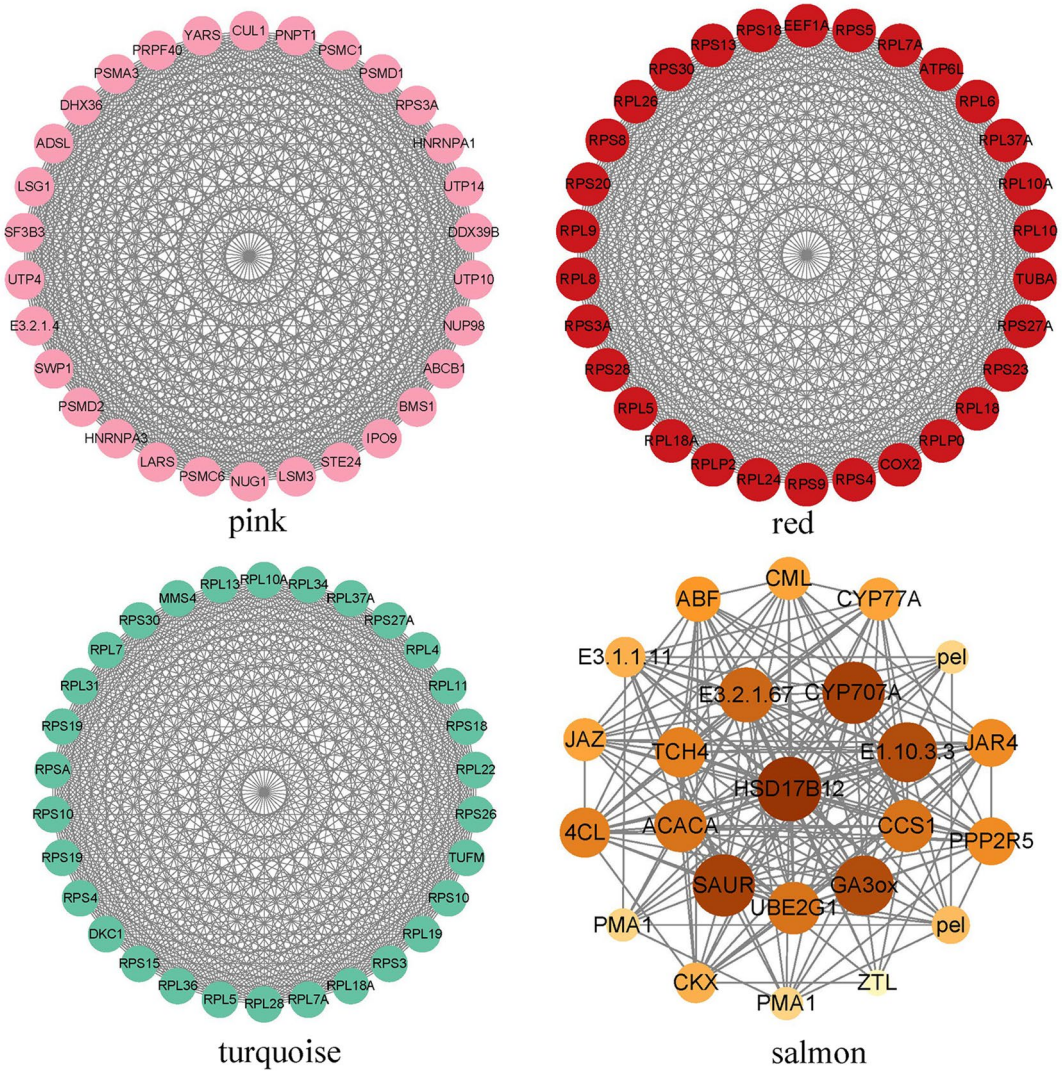

Fig. 14 Coexpression network of hub-genes in top 30 from modules of turquoise, red, pink and salmon

Verification of differential expression gene by quantitative real-time PCR

Twelve differentially expressed genes (DEGs) associated with fruit development were selected for quantitative real-time PCR (qRT-PCR) to validate the gene expression results derived from transcriptomic data. The primers used for qRT-PCR analysis to verify transcriptome data are provided in the supplementary materials (Supplementary Table S7). These DEGs are predominantly implicated in plant hormone signal transduction, sugar transport, and transcription factor activity. The expression patterns of the 12 DEGs, as determined by qRT-PCR, were consistent with those observed in the transcriptomic analysis, thereby corroborating the findings from the transcriptome data (Fig. 15).

Discussion

The process of early fruit development

It is well-established that fruits originate from fertilized ovules, which subsequently develop into mature fruits through a phase characterized by rapid cell division [63]. The onset and duration of the transition phase are variable, contingent upon the time required for pollination and fertilization processes. These processes necessitate ongoing and dynamic interactions between female and male tissues, encompassing multiple stages: pollen hydration, pollen germination, pollen tube growth, pollen tube attraction to the ovule, pollen tube reception, sperm cell delivery, and gamete activation [64]. It has been documented that approximately 48 h post-pollination are required for pollen grains to germinate and release sperm

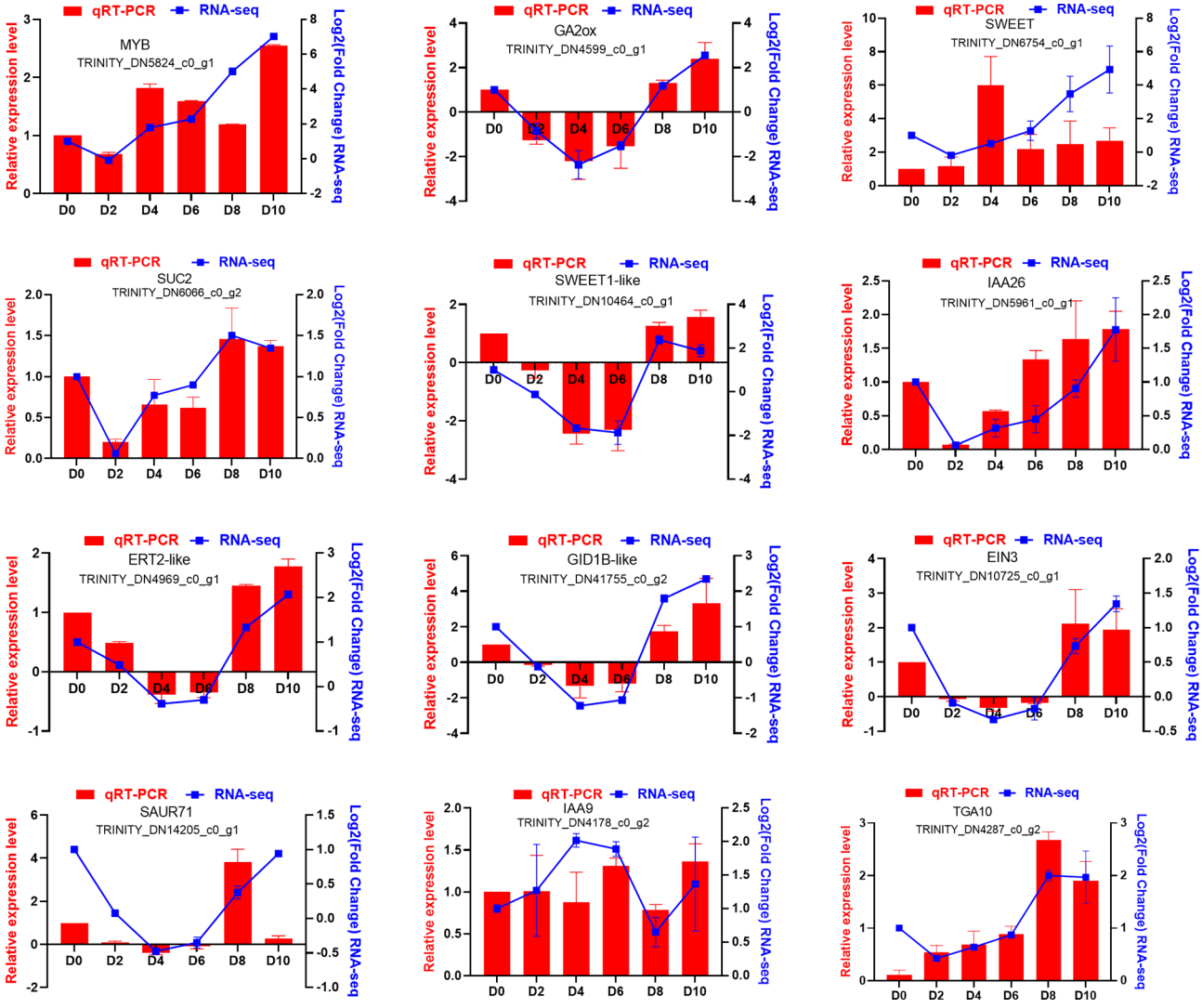

Fig. 15 Relative expression levels of 12 DEGs in ovaries of six time points. MYB, MYB-Type Transcription Factor; GA2ox, Gibberellin 2-beta-dioxygenase; SWEET, SWEET sugar transporter; SUC2, Sucrose transport protein SUC2; SWEET1-like, SWEET sugar transporter; IAA26, Auxin-responsive protein IAA26; ETR2-like, Ethylene receptor 2; GID1B-like, Gibberellin receptor; EIN3, ETHYLENE INSENSITIVE 3; SAUR71, Auxin-responsive protein SAUR71; IAA9, Auxin-responsive protein IAA9; TGA10, bZIP transcription factor TGA10

cells to the ovules in *Actinidia deliciosa* [65]. In this study, observations of pollen tube dynamics indicated that the pollen tubes reached the ovules approximately 48 h post-pollination. Furthermore, the egg and sperm cells were observed to be on the verge of fusion within the embryo sac at 2 days after anthesis (DAA). Consequently, a minimum of 48 h is required for double fertilization in *G. sinensis*. Notably, the egg cell is preferentially fertilized over the polar nucleus [66]. This result corresponded with the nearly unchanged condition of the ovary from 0 days after anthesis (DAA) to 2 DAA, a phenomenon referred to as "ovary arrest " [67]. Following successful fertilization, the ovaries exhibited rapid growth. In this study, morphological changes in the ovaries of *G. sinensis* during early fruit development were notably observed at 6 days after anthesis (DAA), evidenced by significant alterations in fruit length and width compared to the ovaries at 0 DAA. Furthermore, the observed increase in ovary width was primarily attributed to the expansion of the endocarp cell layer and cell volume, as evidenced by paraffin section analysis. This finding suggests that the onset of fruit development in *G. sinensis* occurs at 6 days after anthesis (DAA), coinciding with the readiness of the fertilized polar nucleus for nuclear division and the dormancy of the fertilized egg. This result corroborates previous research indicating that zygote activation is delayed and contingent upon endosperm development [68, 69]. In summary, the early developmental stages of *G. sinensis* fruit can be delineated into two distinct phases: the initial fruit stage, spanning from 0 days after anthesis (DAA) to 4 DAA, and the subsequent rapid cell division stage, commencing at 6 DAA.

Dynamic alterations in non-structural carbohydrate levels within ovaries during the initial stages of fruit development

Carbohydrates, encompassing starch, sucrose, cellulose, glucose, and fructose, serve as essential substances and signaling molecules involved in various processes of plant development and growth. These compounds have been the subject of more extensive study in recent years [70 −74]. Among these investigations, a meticulously designed study on tomatoes demonstrated that fruit set is associated with the activation of central carbon metabolism. This activation is characterized by elevated levels of hexoses, hexose phosphates, and downstream metabolites, including intermediates and derivatives of glycolysis, the tricarboxylic acid cycle, as well as related organic and amino acids [23]. In other studies, elevated concentrations of glucose and fructose, primarily as photoassimilates, were observed during the initial stages of fruit development in zucchini [75]. The reduction of photosynthate through leaf covering inhibited the initiation and growth of parthenocarpic fruits, whereas the exogenous application of sugars markedly promoted parthenocarpic fruit set and growth [30]. In summary, the researchers underscored the pivotal role of carbohydrate metabolism in fruit set and growth. Consequently, sugars can be identified as inductive signals and substances that stimulate fruit development, particularly during the early stages. This study revealed that glucose content in the ovary remained relatively high throughout fruit development, whereas sucrose and fructose content decreased. This phenomenon may be attributed to the maintenance of a high glucose-to-fructose ratio, which is conducive to fruit set. Additionally, it can be partially explained by the elevated regulation of scrK and INV at D0. (Supplementary Figure S4 and Table S8). Sucrose, as a common form of photoassimilate, is typically transported from source to sink tissues in higher plants [76]. Sink strength plays a crucial role in the importation and accumulation of photoassimilates, thereby regulating fruit development and influencing fruit quality [77]. Sucrose synthase is recognized as a key determinant affecting sink strength, as it maintains the sucrose concentration gradient between source and sink, facilitating the loading and transport of sucrose to the sink tissues [78]. In this study, elevated levels of sucrose synthase were observed to enhance sucrose utilization, thereby promoting fruit set and development. This observation aligns with the expression patterns of genes involved in carbohydrate metabolism, such as *SUS* and *scrK*, during the early stages of fruit development. Additionally, variations in ovary starch content could be attributed to the expression patterns of *AMY*, *GEB1*, and *WAXY*. Furthermore, *TPS* genes were identified as being involved in early fruit development, with a notable peak in expression at D4, suggesting a potential role in the fertilization process of *G. sinensis*. Moreover, its function may be realized through its role in regulating sucrose availability and activating auxin biosynthesis, as its downstream product, Trehalose-6-phosphate (T6P), has been demonstrated to act as a signal of sucrose availability [79].

The role of plant hormones in early fruit development

It is well established that plant hormones are integral to fruit set and development [20]. Among these hormones, auxin and gibberellin are particularly recognized for their roles in initiating fruit set and development [19, 22, 80, 81]. In fertilization-dependent plants, the auxin signal in the ovule is activated post-fertilization, which subsequently triggers fruit development by modulating gibberellin metabolism [22]. Then gibberellin or together with other plant hormones, such as auxin, ethylene, stimulate fruit development by regulating metabolic pathways downstream [18, 23, 35, 56]. In this study, various plant hormones, such as auxin, gibberellin, cytokinin, ethylene, jasmonic acid, and salicylic acid, were identified as active

participants in the early fruit development of *G. sinensis*. From the perspective of transcriptional profiling, two distinct modes of gene co-expression associated with plant hormones were observed. The first module exhibited high expression levels before fertilization, which subsequently decreased, with the genes predominantly associated with hormone biosynthesis (Supplementary Figure S3). In contrast, the second module displayed variable expression levels at specific time points, with the genes primarily related to plant hormone signal transduction (Supplementary Figure S4). This study demonstrated that the transcriptional profile associated with plant hormone synthesis and signal transduction was reprogrammed in response to pollination and fertilization, corroborating previous research findings [19, 49]. Specifically, a pattern of auxin, gibberellin, and cytokinin during early fruit development was delineated to elucidate their respective roles (Fig. 16). Consistent with earlier studies, auxin signaling was observed to be initially activated by fertilization [82, 83]. In this investigation, both auxin and its conjugates exhibited an increasing trend, peaking at 6 days after anthesis (DAA), followed by a subsequent decline, although the amount of IAA had no significantly difference among six time points. This observation may suggest that the auxin signaling pathway is activated by fertilization, a hypothesis potentially supported by the expression patterns of auxin-responsive genes such as IAAs, GH3, and ARFs prior to fertilization, which likely initiate negative-feedback loops [84] and the activation of some positive regulatory genes such as, *ARFs* and *SAURs* after fertilization [85]. These genes collectively constitute the auxin regulatory network [42, 61]. Numerous studies have demonstrated that gibberellin plays a crucial role in fruit setting and early fruit development [23, 25, 80]. In the present study, seven types of gibberellins were detected in ovaries during early fruit development, including four bioactive GAs (GA1, GA3, GA4, GA7) and three intermediates or catabolites of bioactive GAs (GA8, GA9, and GA24) [86]. Additionally, the content of all bioactive GAs in the ovaries of *G. sinensis* increased with the number of days post-blossom, with the exception of GA1. The observed increases in the levels of GA3, GA4, and GA7 were accompanied by a decrease in GA2ox transcripts and an increase in GA20ox transcripts at 2DAA, suggesting the activation of gibberellin (GA) biosynthesis and partial suppression of catabolism due to pollination [44]. Conversely, the reduction in GA1 levels is likely attributable to its catabolism, as evidenced by the increased content of GA8, an inactive product of GA1 catabolism [58]. The concurrent rise in GA9 levels alongside bioactive GAs can be attributed to the elevated expression of GA20ox and GA3ox [87]. The important

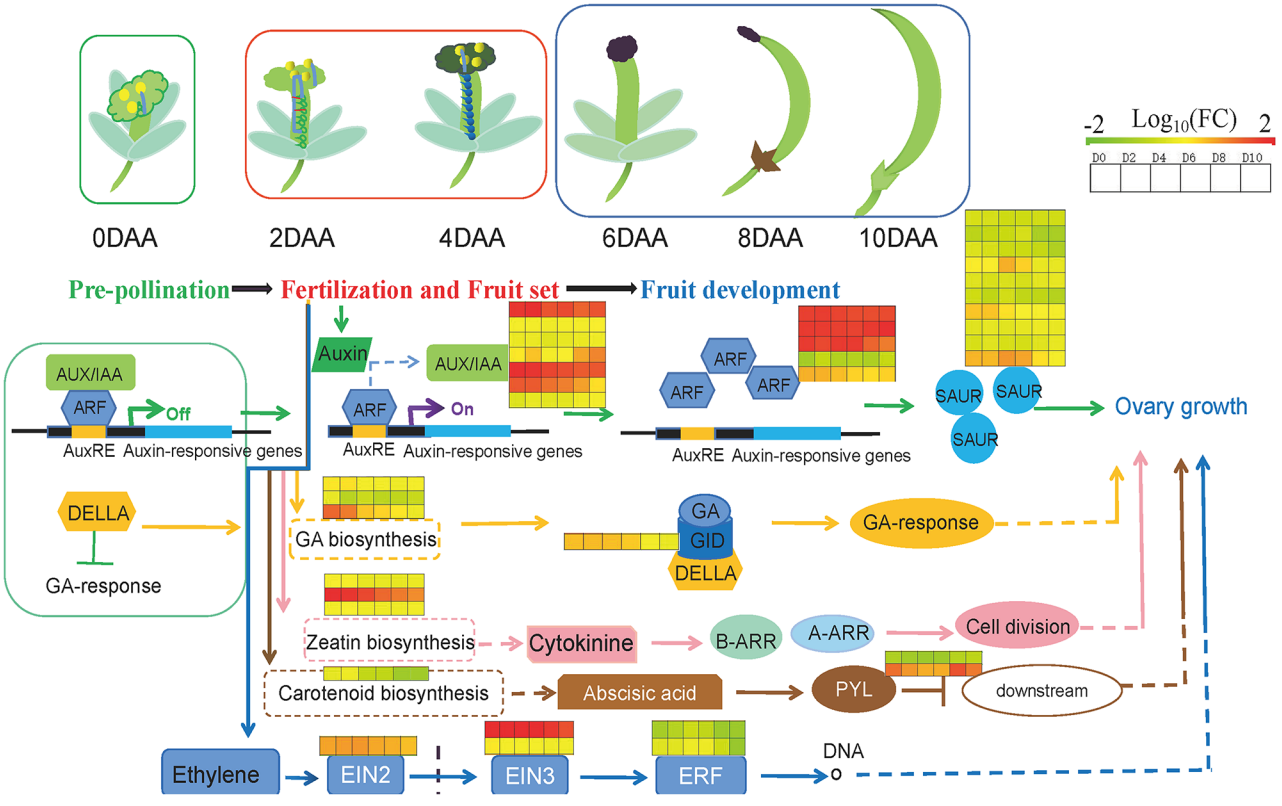

Fig. 16 Hormone signaling pathway map in early fruit development of *G. sinensis*

role that cytokinine played during early fruit development could be explained by several studies about exogenous application of cytokinin inducing parthenocarpy [88]. Despite the hormonal interactions, the activated cytokinin biosynthesis after pollination and fertilization was undisputed based on the KEGG enrichment analysis (Fig. 13). After that, its signal was transmitted to downstream, result in cell division. Furthermore, some studies showed that ethylene and abscisic acid also played a major role in fruit setting, especially reflected in the maintenance of the ovary state before fertilization [35, 48, 49]. In this research, genes not only related to ethylene and abscisic acid signal transduction, such as EIN3 and ABF, but also related to jasmonic acid, salicylic acid and brassinoids, like JAZ, JAR1_4_6, CYP85A1, WRKY22 all co-expressed during the early fruit development. The ovary content of ACC, ABA, SA and JA, which were generally considered as stress-related hormones, showed a trend of increase from 0 DAA to 2 or 4 DAA and then decrease after that. Thus, the results indicated that these stress-related hormones and their related genes probably participated in maintaining the quiescent status of ovary prior to fertilization and may be involved in cell-to-cell recognition signals during double fertilization [50]. Although we found some transcript associated with brassinoids, like CYP90, CYP85 and BSK, the content of brassinoids in ovaries were undetected, which showed that there could be functional redundancy between brassinoids and other hormones [60, 89]. To sum up, plant hormones and their signal transduction processes constituted a complex regulatory network involved in early fruit development of *G. sinensis*.

Conclusions

This study precisely delineated the initiation and subsequent development of *G. sinensis* during its early fruit development stages. Concurrently, it enhanced our comprehension of the alterations in non-structural carbohydrates and phytohormone dynamics during this period, as well as the transcriptional landscape underpinning these changes. Utilizing this data, we elucidated the intricately programmed complex regulatory network operative during early fruit development, thereby offering a valuable resource for functional studies on early fruit development and molecular breeding aimed at improving fruit set.

Methods

Collection of experimental materials

Field experiments were conducted at the planting base in Guiyang, Guizhou Province (26°45′ N, 106°56′ E) from March to May 2022. The site experiences an annual average temperature of 15.7℃ and an annual precipitation of 1215.7 mm. Six 12-year-old female plants, characterized by consistent growth and stable flowering, were selected from the plantations to observe their flowering dynamics. Approximately 2000 perfect flowers were labeled at the bud stage. To ensure successful pollination, each flower was artificially pollinated on the day it bloomed. Subsequently, the labeled flowers were categorized into six stages based on the time elapsed after pollination: 0 days (0d), 2 days (2d), 4 days (4d), 6 days (6d), 8 days (8d), and 10 days (10d). For each stage, 30 ovaries from the labeled flowers were randomly selected to measure their length, width, and thickness. Additionally, 600 labeled ovaries from each stage were collected, immediately frozen in liquid nitrogen after the corolla was removed using tweezers, and then stored at -80 °C for transcriptome sequencing and endogenous hormone content analysis and physiological indicators measurement.

Scanning electron microscopy of the stigma

To examine the morphological changes in stigma mastoid cells using scanning electron microscopy (SEM), ovaries labeled at six different time points were fixed in glutaraldehyde for 24 h. Subsequently, the fixed and dissected samples underwent a dehydration process through a graded ethanol series, followed by an acetone series: 30%, 50%, 70%, 80%, 90%, and 100% ethanol for 15 min each, then ethanol/acetone (1:1, v/v) for 30 min, and finally 100% acetone for 30 min. The samples were then subjected to critical-point drying using liquid CO2 (Emitech K850, UK). Afterward, all samples were sputter-coated with gold and examined using a scanning electron microscope running at an accelerating voltage of 3 kV (Hitachi, Japan).

Observation of pollen tube dynamics

To investigate pollen tube dynamics during early fruit development, ovaries at six developmental stages were labeled and fixed by immersion in a fixative solution composed of 70% ethanol, formaldehyde, and acetic acid in a ratio of 90:5:5 for 24 h. Following fixation, the ovaries were rinsed three times with distilled water and subsequently incubated in a 2 mol/L sodium hydroxide solution at 60 °C for 6 h to facilitate softening. The softened ovaries were then stained with a 0.1% Aniline blue solution. Post-staining, the ovaries were prepared for microscopic examination using a temporary squash technique and observed under a fluorescence microscope (Leica DM3000), where they were also photographed.

Paraffin embedding, sectioning

To elucidate the microscopic characteristics of the ovary during early fruit development, ovaries at six developmental stages were labeled and fixed by immersion in a fixative solution composed of 70% ethanol, formaldehyde, and acetic acid in a ratio of 90:5:5 for 24 h. Subsequently,

the fixed ovaries underwent a dehydration process using a graded ethanol series (30%, 50%, 70%, 85%, 95%, and 100%) for 40 min each at room temperature. The tissue was then infiltrated with xylene through an ethanol-xylene series (1:1, 0:1, 0:1, and 0:1) at room temperature. Xylene was gradually substituted with molten paraffin through a series of xylene: paraffin mixtures (1:1, 0:1, and 0:1) for 3 h each at 60 °C. The paraffin-embedded tissue was subsequently sectioned into 8-μm thick slices using a microtome and mounted on polylysine-coated slides. The sections were dewaxed by immersion in xylene, followed by rehydration through a graded ethanol series (100%, 95%, 85%, 70%, 50%) for Safranin O staining. For Fast Green staining, the sections were dehydrated using a graded ethanol series (50%, 70%, 85%, 95%). After the application of the stain, the slides were permanently mounted using Neutral Balsam and a cover slip. The prepared slides were then observed and photographed under a microscope (Leica DM2500).

Physiological analyses

Sucrose, fructose and glucose measurements

Ovarian samples, each weighing 100 mg, were collected at various time points for the extraction of sucrose, fructose, and glucose using the Hexokinase method. The detailed protocol followed is provided by the test kit (www.geruisi-bio.com G0545W). The absorbance of the reactants was measured at 340 nm using an ultraviolet-visible (UV-Vis) spectrophotometer (SPARK).

Soluble sugar

100 mg ovaries at different stages were used to extract soluble sugar. The detailed procedure was according to the test kit (www.geruisi-bio.com G0501W).The absorption values of the reactant were measured under 620 nm ultraviolet light by Ultraviolet-uv accounting protein detector (SPARK).

Soluble acid invertase (S-AI) and neutral invertase (NI) activity

100 mg ovaries at different stages were used to extract S-AI and NI. The detailed procedure is according to the test kit (www.geruisi-bio.com G0517W and G0516W). The absorption values of the reactant were measured under 540 nm ultraviolet light by Ultraviolet-uv accounting protein detector (SPARK).

Sucrose synthase EC2.4.1.13 (SS-I) and (SS-II) activity

100 mg ovaries at different stages were used to extract SS-I and SS-II. The detailed procedure is according to the test kit (www.geruisi-bio.com G0513W and G0512W). The absorption values of the reactant were measured under 480 nm ultraviolet light by Ultraviolet-uv accounting protein detector (SPARK).

Targeted metabolomics of plant hormone

Plant hormone standard solution preparation

An appropriate quantity of 46 standard plant hormones was precisely weighed and dissolved in methanol, with the volume adjusted to 1 mL. The solution was vortex-mixed to obtain a standard stock solution. The concentration details of the stock solution are as follows: The aforementioned standard stock solution was mixed according to specified concentrations and subsequently diluted with 50% methanol-water to prepare working solutions labeled C1 through C10. These working solutions were then transferred into 1.5 mL Eppendorf tubes.

Sample treatment

A 200 mg sample was precisely weighed, and 1 mL of a 5% ammonia water methanol solution was added. The mixture was subjected to ultrasound treatment at a low temperature (5℃, 40 kHz) for 60 min. Subsequently, the sample was centrifuged at 4℃ for 15 min at 14,000 rcf. A 500 uL aliquot of the supernatant was then transferred to a MAX 96-well plate with 30 μm pore size for enrichment and purification. The collected flow-through and eluent were transferred to a 2 mL centrifuge tube for nitrogen evaporation. Once dried, 100uL of a 50% methanol aqueous solution was added, thoroughly mixed via vortexing, and subjected to ultrasonic extraction at a low temperature (5℃, 40 kHz) for 5 min. Ultimately, the liquid supernatant was transferred into the sample vial following centrifugation at 4 °C for 15 min at 14,000 relative centrifugal force (rcf).

LC-MS detection

In this experiment, qualitative and quantitative detection of the target analyte in the sample was performed using LC-ESI-MS/MS (UHPLC-Qtrap). The specific parameters were as follows: Chromatographic conditions utilized an ExionLC AD system with an Agilent Poroshell 120 EC-C18 column (3.0×100 mm, 1.9 μm). The column temperature was maintained at 30 °C, and the injection volume was 10 μL. The mobile phase consisted of two components: mobile phase A (5 mM ammonium formate with 0.05% formic acid in water) and mobile phase B (5 mM ammonium formate with 0.05% formic acid in methanol).

Mass spectrometry conditions were as follows: AB SCIEX QTRAP 6500+was utilized in both positive and negative mode detection. The Curtain Gas (CUR) was set at 35, and the Collision Gas (CAD) was set to medium. The IonSpray Voltage (IS) was configured to +5500 V for positive mode and −4500 V for negative mode. The Temperature (TEM) was maintained at 550 °C, while Ion Source Gas1 (GS1) and Ion Source Gas2 (GS2) were both set at 50. Ion fragments were automatically identified and integrated using the default parameters in the AB

Sciex quantitative software OS, supplemented by manual inspection. A standard linear regression curve was constructed, with the mass peak area of the analyte plotted on the ordinate and the concentration of the analyte on the abscissa. Calculation of Sample Concentration: The mass peak area of the analyte within the sample was incorporated into the linear regression equation to determine the concentration.

Transcriptome sequencing

RNA extraction, libraries preparation, and sequencing

Ovarian samples collected at six distinct time points and stored at -80℃ were utilized for RNA extraction and subsequent sequencing, conducted by Majorbio Company in Shanghai, China (www.majorbio.com). Total RNA was extracted using the TRIzol reagent kit. The concentration, purity, and integrity of the extracted RNA were assessed using a Nanodrop2000 spectrophotometer and agarose gel electrophoresis. Following these assessments, RNA samples were enriched with OligodTs and randomly fragmented by the addition of fragmentation buffer. Under the catalytic activity of reverse transcriptase, six-base random hexamers were utilized to synthesize single-stranded cDNA using mRNA as a template. Subsequently, a stable double-stranded structure was achieved through double-strand synthesis. The resultant double-stranded cDNA underwent purification processes, including end-repair, A-tailing, and ligation with sequencing adapters. The final cDNA libraries were generated through size selection and PCR enrichment reactions. These libraries were then pooled and sequenced using the NovaSeq 6000 platform (Illumina, San Diego, CA, USA).

Sequencing data analyses

The sequencing data underwent processing, during which the sequencing error rate and GC content distribution were assessed following a quality check of the raw data. Reads containing adaptors, paired reads, and low-quality reads were excluded. Upon obtaining high-quality sequencing data, all clean data were reassembled using Trinity (Version v2.8.5, https://github.com/trinityrnaseq/trinityrnaseq). The longest transcript post-assembly was designated as the unigene for reference sequences in subsequent analyses. The unigenes were then used for blast to compare the unigene sequences with different annotation databases including NR (Version 2021.10, https://www.ncbi.nlm.nih.gov/public/), Pfam (Version 34.0, http://pfam.xfam.org/), SwissProt (Version 2021.06, http://www.ftp.uniprot.org/pub/databases/uniprot/current_release/knowledgebase/complete/uniprot_sprot.fasta.gz), KEGG (Version 2021.09, http://www.genome.jp/kegg/), and GO (Version 2021.0918, http://www.geneontology.org/). The TPM (Transcripts per Million Reads) values were determined using the RSEM for each replicate of groups (Version 1.3.1, http://deweylab.biostat.wisc.edu/rsem/). DEGs (defined as log2 fold change > 1or <–1, adjusted P-value < 0.05) analysis by DESeq2 was used in comparison with the expression of genes between ovaries of any two time points across early fruit developmental stages [90].

qRT-PCR

To validate the RNA-seq data, the expression levels of 12 differentially expressed genes (DEGs) were assessed using quantitative reverse transcription PCR (qRT-PCR). Reverse transcription was performed with the TURE-script 1st Strand cDNA Synthesis Kit (Aidlab, Beijing, China). The primers used for qRT-PCR are detailed in Table S1. The qRT-PCR reaction mixture comprised 10 uL of 2×SYBR® Green Supermix, 0.5 uL of each primer, 1uL of diluted cDNA, and 8uL of double-distilled water. PCR amplification was carried out under the following conditions: an initial denaturation at 95 ℃ for 3 min, followed by 39 cycles of 95 ℃ for 10 s and 60℃ for 30 s. The relative expression levels of the DEGs were determined using the $2^{-\Delta\Delta CT}$ method.

Statistical analysis

The collected data were analyzed utilizing analysis of variance (ANOVA), and mean comparisons were conducted using a t-test within the SPSS 17.0 software (SPSS Inc., Chicago, IL, USA). Statistical significance was determined at a threshold of $P < 0.05$. Figures were generated using GraphPad Prism 9.3 (GraphPad Software, LLC) and RStudio (Version 4.2.3).

Abbreviations

DAA	Days after anthesis
SSI	Sucrose synthase (resultant direction)
SSII	Sucrose synthase (decomposition direction)
NI	Neutral invertase
AI	Acid invertase
HPLC-MS/MS	High-performanceliquid chromatographytandem mass spectrometry
IAA	Indole-3-acetic acid
IAAsp	Indole-3-acetyl-l-aspartic acid
IAAla	Indole-3-acetyl-L-alanine
tZR	Trans-zeatin nucleotide
GA	Gibberellin
SA	Salicylicacid
JA	Jasmonicacid
ABA	Abscisic acid
ACC	1-aminocyclopropane carboxylic acid
DEGs	different expressed genes
GO	Gene Ontology
KEGG	Kyoto Encyclopedia of Genes and Genomes
WGCNA	Weighted correlation network analysis
GA2ox	Gibberellin 2-beta-dioxygenase gene
MAPKKK	Mitogen-activated protein cascade kinas ecoding gene
WRKY	WRKY transcription factor
CYP	Cytochrome P450 gene
CCS	Capsanthin/Capsorubin synthase gene
SAUR	Small auxin up RNA
ABF	ABRE binding factor

GA3ox	Gibberellin 3-beta-dioxygenase gene
ARF	Auxin response factor
AUX/IAA	Auxin/Indole-3Acetic coding gene
AUX1	Auxin efflux carrier coding gene
GH3	Primary-response genes
JAZ	Jasmonate ZIM-domain coding gene
EIN3	Ethylene insensitive 3
ERF	Ethylene response factor
PYL	Abscisic acid receptor gene
BSK	Serine/threonine-protein kinase coding gene
TGA	TGA transcription factor
DELLA	Gibberellin negative regulatory protein coding gene
ARR	Arrestin
AHP	Histidine phosphate transporter coding gene
SNRK2	Ser/Thr protein kinase coding gene
RPS	Small subunit of ribosomal protein coding gene
RPL	Large subunit of ribosomal protein coding gene
DHX36	Helicase gene
LARS	Leucoyl-trna synthetase gene
PNPT1	Polyribonucleotide transferase 1 gene
PPP2R5	Protein phosphatase 2 coding gene
UBE2G1	Ubiquitin-binding enzyme E2G1 coding gene
E1.10.3.3	Corbate oxidase
E3.2.1.67	galacturan 1,4-alpha-galacturonidase
E3.1.1.11	Pectinesterase
SUS	Sucrose synthase coding gene
scrK	Sucrose metabolizing enzymes coding gene
AMY	Amylase coding gene
GEB1	Beta-galactosidase gene
WAXY	Granulated starch synthetase gene
TPS	Trehalose synthase gene

Supplementary Information

The online version contains supplementary material available at https://doi.org/10.1186/s12870-024-05895-8.

Supplementary Material 1

Supplementary Material 2

Supplementary Material 3

Supplementary Material 4

Supplementary Material 5

Supplementary Material 6

Supplementary Material 7

Supplementary Material 8

Supplementary Material 9

Acknowledgements
Not applicable.

Author contributions
QL and XW conceived and coordinated the study; QL and JY performed experiments; QL performed data analysis, prepared figures, and wrote the article; QL and FX contributed to bioinformatic data analysis, drafting the figures and tables; YZ and XW contributed to materials, reagents and article revision. All authors read and approved the final article.

Funding
This work was supported by the Characteristic Forestry Industry Research Project of Guizhou Province(GZMC-ZD20202098, GZMC-ZD20202102), the China National Key R&D Program (Grant No. 2022YFD1601712-1) and the Science and Technology Plan Project of Guizhou Province ([2022] general 102).

Data availability
The RNA-seq data are available from the SRA database under the accession number PRJNA972499. The datasets used and/or analysed during the current study are available from the corresponding author on reasonable request.

Declarations

Ethics approval and consent to participate
Not applicable.

Consent for publication
Not applicable.

Competing interests
The authors declare no competing interests.

Received: 1 September 2023 / Accepted: 29 November 2024
Published online: 19 December 2024

References

1. Yang Y, Liu X-L, Lu X, Sun Q-W. Ecological suitability zoning of *Gleditsia sinensis* in China based on MaxEnt and ArcGIS. Shi Zhen Chin Med. 2022;33:1201–4.
2. Lan Y-P, Zhou L-D, Li S-Y, Cao Q-C, Lan W-Z. Research progress and industrialization prospect of *Gleditsia sinensis*(*Gleditsia*). World Forestry Res. 2004;17:17–21.
3. Zhang T, Jiang H-H, Jiang W, Zhang H-W, Song X-S, Deng C. Research progress of *Gleditsia sinensis*. Wild Plant Resour China. 2021;40:46–54.
4. Shin TY, Kim DK. Inhibitory effect of mast cell-dependent anaphylaxis byGleditsia sinensis. Arch Pharm Res. 2000;23:401–6.
5. Kim KH, Kwun MJ, Han CW, Ha K-T, Choi J-Y, Joo M. Suppression of lung inflammation in an LPS-induced acute lung injury model by the fruit hull of Gleditsia sinensis. BMC Complement Altern Med. 2014;14:402.
6. Li J-J, Ye C-L, Shang X-C, Wang J, Zhang B, Wang Z-Z, Zhang G-T. Study on breeding system and pollination characteristics of *Gleditsia sinensis*. Chin J Traditional Chin Med. 2018;43:4831–6.
7. Yu Z-Y, Yan H-B, Zhang H-F, Yang. X-Q.Effects of different salt stress on seed germination and seedling physiological characteristics of Gleditsia sinensis. J Northeast Agricultural Univ. 2021;51:28–35.
8. Zhu L-W, Hang Z-J, Jiang J-X, Zhang W-M, An X-N, Gan. X-H.Comparison of microstructures of endosperm cells of five legume seeds. Wild Plant Resour China. 2003;22:62–6.
9. Li L-H. Analysis of the economic utilization value and market prospect of *Gleditsia sinensis* and the existing problems and strategies in its development. Mod Hortic. 2018;3:22–3.
10. Yu J, Li G, Mu Y, Zhou H, Wang X, Yang P. Anti-breast cancer triterpenoid saponins from the thorns of *Gleditsia sinensis*. Nat Prod Res. 2019;33:2308–13.
11. Zhang H, Zhang Y, Wang Y, Zhan R, Chen Y. A new neolignan from the thorns of *Gleditsia japonica var. Delavayi*. Nat Prod Res. 2019;33:239–43.
12. Zhang C-J, Zhao. X-B.Market research and reflection on the cultivation and industry of *Gleditsia sinensis* in Yunnan and Guizhou Province. Mod Hortic. 2021;44:23–4.
13. Yang X-J, Zhao X-B, Li. L-H.Development status and countermeasures of *Gleditsia sinensis* industry in Songxian. Mod Gardening. 2020;43:12–4.
14. Kambal AE. Flower drop and fruit set in field beans, *Vicia faba* L. J Agric Sci. 1969;72:131–8.
15. Fan Y-F, Jiang L, Gong H-Q, Liu C-M. Sexual Reproduction in higher plants I: fertilization and the Initiation of Zygotic Program. J Integr Plant Biol. 2008;50:860–7.
16. Ma C, Meir S, Xiao L, Tong J, Liu Q, Reid MS, et al. A KNOTTED1-LIKE HOMEOBOX protein regulates Abscission in Tomato by modulating the Auxin Pathway. Plant Physiol. 2015;167:844–53.
17. Tornielli GB, Sandri M, Fasoli M, Amato A, Pezzotti M, Zuccolotto P, et al. A molecular phenology scale of grape berry development. Hortic Res. 2023;10:uhad048.
18. An J, Althiab Almasaud R, Bouzayen M, Zouine M, Chervin C. Auxin and ethylene regulation of fruit set. Plant Sci. 2020;292:110381.
19. Zhang S, Gu X, Shao J, Hu Z, Yang W, Wang L, et al. Auxin metabolism is involved in Fruit Set and early Fruit Development in the Parthenocarpic Tomato R35-P. Front Plant Sci. 2021;12:671713.

20. Vriezen WH, Feron R, Maretto F, Keijman J, Mariani C. Changes in tomato ovary transcriptome demonstrate complex hormonal regulation of fruit set. New Phytol. 2008;177:60–76.
21. Luo W, Li Y, Sun Y, Lu L, Zhao Z, Zhou J, et al. Comparative RNA-seq analysis reveals candidate genes associated with fruit set in pumpkin. Sci Hortic. 2021;288:110255.
22. Dorcey E, Urbez C, Blázquez MA, Carbonell J, Perez-Amador MA. Fertilization-dependent auxin response in ovules triggers fruit development through the modulation of gibberellin metabolism in Arabidopsis. Plant J. 2009;58:318–32.
23. Shinozaki Y, Beauvoit BP, Takahara M, Hao S, Ezura K, Andrieu M-H, et al. Fruit setting rewires central metabolism via gibberellin cascades. Proc Natl Acad Sci. 2020;117:23970–81.
24. Kang C, Darwish O, Geretz A, Shahan R, Alkharouf N, Liu Z. Genome-scale transcriptomic insights into early-stage Fruit Development in Woodland Strawberry Fragaria vesca. Plant Cell. 2013;25:1960–78.
25. Serrani JC, Ruiz-Rivero O, Fos M, García-Martínez JL. Auxin-induced fruit-set in tomato is mediated in part by gibberellins. Plant J. 2008;56:922–34.
26. Figueiredo DD, Batista RA, Roszak PJ, Köhler C. Auxin production couples endosperm development to fertilization. Nat Plants. 2015;1:15184.
27. Gupta SK, Barg R, Arazi T, Tomato. *agamous-like6* parthenocarpy is facilitated by ovule integument reprogramming involving the growth regulator *KLUH*. Plant Physiol. 2021;185:969–84.
28. Tian Y, Chen Z, Jiang Z, Huang X, Zhang L, Zhang Z et al. Effects of Plant Growth Regulators on Flower Abscission and Growth of Tea Plant Camellia sinensis (L.) O. Kuntze. J Plant Growth Regul. 2021. https://doi.org/10/gnpnr7.
29. Wang T, Liu Q, Wang N, Dai J, Lu Q, Jia X, et al. Foliar arginine application improves tomato plant growth, yield, and fruit quality via nitrogen accumulation. Plant Growth Regul. 2021. https://doi.org/10/gm3ksq.
30. Wang M, Su L, Cong Y, Chen J, Geng Y, Qian C, et al. Sugars enhance parthenocarpic fruit formation in cucumber by promoting auxin and cytokinin signaling. Sci Hortic. 2021;283:110061.
31. Cheng J, Chen H, Ding X, Shen T, Peng Z, Kong Q, et al. Transcriptome analysis of the influence of CPPU application for fruit setting on melon volatile content. J Integr Agric. 2021;20:3199–208.
32. Time A, Ponce C, Kuhn N, Arellano M, Sagredo B, Donoso JM, et al. Canopy spraying of Abscisic Acid to Improve Fruit Quality of different Sweet Cherry cultivars. Agronomy. 2021;11:1947.
33. Carra B, Herter FG, Moretti Ferreira Pinto FA, Fontanella Brighenti A, Pereira Pasa C, Mello-Farias PC, et al. Return Bloom and Yield of 'Rocha' Pear Trees are improved by Ethephon and Paclobutrazol. J Plant Growth Regul. 2022. https://doi.org/10.1007/s00344-022-10827-7.
34. Xu F, Xi Z, Zhang H, Zhang C, Zhang Z. Brassinosteroids are involved in controlling sugar unloading in Vitis vinifera 'Cabernet Sauvignon' berries during véraison. Plant Physiol Biochem. 2015;94:197–208.
35. Shinozaki Y, Hao S, Kojima M, Sakakibara H, Ozeki-Iida Y, Zheng Y, et al. Ethylene suppresses tomato (*Solanum lycopersicum*) fruit set through modification of gibberellin metabolism. Plant J. 2015;83:237–51.
36. Silva EM, Silva GFF e, Bidoia DB, Silva Azevedo M, Jesus FA, Pino LE et al. micro RNA 159-targeted *SlGAMYB* transcription factors are required for fruit set in tomato. Plant J. 2017;92:95–109.
37. Hu J, Israeli A, Ori N, Sun T. The Interaction between DELLA and ARF/IAA mediates crosstalk between Gibberellin and Auxin Signaling to Control Fruit Initiation in Tomato. Plant Cell. 2018;30:1710–28.
38. Srivastava A, Handa AK. Hormonal regulation of Tomato Fruit Development: a molecular perspective. J Plant Growth Regul. 2005;24:67–82.
39. Gessler A. Sucrose synthase – an enzyme with a central role in the source–sink coordination and carbon flow in trees. New Phytol. 2021;229:8–10.
40. Wang F, Sanz A, Brenner ML, Smith A. Sucrose synthase, Starch Accumulation, and Tomato Fruit Sink Strength. Plant Physiol. 1993;101:321–7.
41. Coluccio Leskow C, Conte M, del Pozo T, Bermúdez L, Lira BS, Gramegna G, et al. The cytosolic invertase NI6 affects vegetative growth, flowering, fruit set, and yield in tomato. J Exp Bot. 2021;72:2525–43.
42. Casanova-Sáez R, Mateo-Bonmatí E, Ljung K. Auxin metabolism in plants. Cold Spring Harb Perspect Biol. 2021;13:a039867.
43. Bon DJ-YD, Mander LN, Lan P. Syntheses of Gibberellins A_{15} and A_{24}, the Key metabolites in Gibberellin Biosynthesis. J Org Chem. 2018;83:6566–72.
44. Olszewski N, Sun T, Gubler F. Gibberellin Signaling. Plant Cell. 2002;14(suppl 1):S61–80.
45. Carbonell-Bejerano P, Urbez C, Granell A, Carbonell J, Perez-Amador MA. Ethylene is involved in pistil fate by modulating the onset of ovule senescence and the GA-mediated fruit set in Arabidopsis. BMC Plant Biol. 2011;11:84.
46. Gomi K. Jasmonic Acid pathway in plants 2.0. Int J Mol Sci. 2021;22:3506.
47. Janda T, Szalai G, Pál M. Salicylic acid signalling in plants. Int J Mol Sci. 2020;21:2655.
48. Shinozaki Y, Ezura H, Ariizumi T. The role of ethylene in the regulation of ovary senescence and fruit set in tomato (*Solanum lycopersicum*). Plant Signal Behav. 2018;13:e1146844.
49. Zhang XS, O'Neill SD. Ovary and Gametophyte Development are Coordinately regulated by Auxin and Ethylene following pollination. Plant Cell. 1993;:403–18.
50. Zakharova EV, Khaliluev MR, Kovaleva LV. Hormonal Signaling in the Progamic phase of fertilization in plants. Horticulturae. 2022;8:365.
51. Huang J, Yang L, Yang L, Wu X, Cui X, Zhang L, et al. Stigma receptors control intraspecies and interspecies barriers in Brassicaceae. Nature. 2023;614:303–8.
52. Robinson R, Sprott D, Couroux P, Routly E, Labbé N, Xing T, et al. The triticale mature pollen and stigma proteomes – assembling the proteins for a productive encounter. J Proteom. 2023;278:104867.
53. Wang L, Lau Y-L, Fan L, Bosch M, Doughty J. Pollen Coat proteomes of Arabidopsis thaliana, Arabidopsis lyrata, and Brassica oleracea Reveal Remarkable Diversity of Small Cysteine-Rich proteins at the Pollen-Stigma Interface. Biomolecules. 2023;13:157.
54. Langfelder P, Horvath S. WGCNA: an R package for weighted correlation network analysis. BMC Bioinformatics. 2008;9:559.
55. Shi S, Li D, Li S, Wang Y, Tang X, Liu Y, et al. Comparative transcriptomic analysis of early fruit development in eggplant (Solanum melongena L.) and functional characterization of SmOVATE5. Plant Cell Rep. 2023. https://doi.org/10.1007/s00299-022-02959-7.
56. He H, Yamamuro C. Interplays between auxin and GA signaling coordinate early fruit development. Hortic Res. 2022;9:uhab078.
57. Pattison RJ, Csukasi F, Zheng Y, Fei Z, van der Knaap E, Catalá C. Comprehensive Tissue-Specific Transcriptome Analysis Reveals Distinct Regulatory Programs during early Tomato Fruit Development. Plant Physiol. 2015;168:1684–701.
58. Gil J, García-Martinez JL. Light regulation of gibberellin A_1 content and expression of genes coding for GA 20-oxidase and GA 3β -hydroxylase in etiolated pea seedlings. Physiol Plant. 2000;108:223–9.
59. Kawade K, Li Y, Koga H, Sawada Y, Okamoto M, Kuwahara A, et al. The cytochrome P450 CYP77A4 is involved in auxin-mediated patterning of the*Arabidopsis thaliana*embryo. Development. 2018;145:dev168369.
60. Nomura T, Bishop GJ. Cytochrome P450s in plant steroid hormone synthesis and metabolism. Phytochem Rev. 2006;5:421–32.
61. Rozov SM, Zagorskaya AA, Deineko EV, Shumny VK. Auxins: biosynthesis, metabolism, and transport. Biol Bull Rev. 2013;3:286–95.
62. van Mourik H, van Dijk ADJ, Stortenbeker N, Angenent GC, Bemer M. Divergent regulation of Arabidopsis SAUR genes: a focus on the SAUR10-clade. BMC Plant Biol. 2017;17:245.
63. Rajewski A, Maheepala DC, Le J, Litt A. Multispecies transcriptomes reveal core fruit development genes. Front Plant Sci. 2022;13:954929.
64. Cascallares M, Setzes N, Marchetti F, López GA, Distéfano AM, Cainzos M, et al. A complex journey: cell wall remodeling, interactions, and Integrity during Pollen Tube Growth. Front Plant Sci. 2020;11:599247.
65. Qi X-J, Xu S-K, Zhang W-Y, LinM-M, Fang J-B. Studies on compatibility of interspecific hybridization between Actinidia diliciosa'Xuxiang'and A. longicarpa by anatomy. Acta Hortic Sin. 2013;40:1897–904.
66. Li L, Hou S, Xiang W, Song Z, Wang Y, Zhang L, et al. The egg cell is preferentially fertilized in *Arabidopsis* double fertilization. J Integr Plant Biol. 2022;64:2039–46.
67. Gillaspy G, Ben-David H, Gruissem W. Fruits: a developmental perspective. Plant Cell. 1993;:1439–51.
68. Xiong H, Wang W, Sun M-X. Endosperm development is an autonomously programmed process independent of embryogenesis. Plant Cell. 2021;33:1151–60.
69. Friedman WE, Bachelier JB, Hormaza JI. Embryology in *Trithuria submersa* (Hydatellaceae) and relationships between embryo, endosperm, and perisperm in early-diverging flowering plants. Am J Bot. 2012;99:1083–95.
70. Mishra BS, Sharma M, Laxmi A. Role of sugar and auxin crosstalk in plant growth and development. Physiol Plant. 2022;174.
71. Zhai Z, Keereetaweep J, Liu H, Xu C, Shanklin J. The role of Sugar Signaling in regulating plant fatty acid synthesis. Front Plant Sci. 2021;12:643843.
72. Wingler A, Henriques R. Sugars and the speed of life—metabolic signals that determine plant growth, development and death. Physiol Plant. 2022;174.
73. Narutaki A, Kahar P, Shimadzu S, Maeda S, Furuya T, Ishizaki K et al. Sucrose signaling contributes to the maintenance of vascular cambium by inhibiting cell differentiation. Plant Cell Physiol. 2023;:pcad039.

74. Kabeya D, Han Q. Seasonal patterns of sugar components and their functions in branches of *Fagus crenata* in association with three reproduction events. Ecol Res. 2022;:1440–703.12370.
75. Pomares-Viciana T, Del Río-Celestino M, Román B, Die J, Pico B, Gómez P. First RNA-seq approach to study fruit set and parthenocarpy in zucchini (Cucurbita pepo L). BMC Plant Biol. 2019;19:61.
76. White AC, Rogers A, Rees M, Osborne CP. How can we make plants grow faster? A source–sink perspective on growth rate. J Exp Bot. 2016;67:31–45.
77. Li Y-M, Forney C, Bondada B, Leng F, Xie Z-S. The Molecular Regulation of Carbon Sink Strength in Grapevine (Vitis vinifera L). Front Plant Sci. 2021;11:606918.
78. Fedosejevs ET, Feil R, Lunn JE, Plaxton WC. The signal metabolite trehalose-6-phosphate inhibits the sucrolytic activity of sucrose synthase from developing castor beans. FEBS Lett. 2018;592:2525–32.
79. Meitzel T, Radchuk R, McAdam EL, Thormählen I, Feil R, Munz E, et al. Trehalose 6-phosphate promotes seed filling by activating auxin biosynthesis. New Phytol. 2021;229:1553–65.
80. Mesejo C, Yuste R, Reig C, Martínez-Fuentes A, Iglesias DJ, Muñoz-Fambuena N, et al. Gibberellin reactivates and maintains ovary-wall cell division causing fruit set in parthenocarpic Citrus species. Plant Sci. 2016;247:13–24.
81. Pandolfini T, Molesini B, Spena A. Molecular dissection of the role of auxin in fruit initiation. Trends Plant Sci. 2007;12:327–9.
82. Goetz M, Vivian-Smith A, Johnson SD, Koltunow AM. *AUXIN RESPONSE FACTOR8*Is a Negative Regulator of initiationiation in*Arabidopsis*. Plant Cell. 2006;18:1873–86.
83. de Jong M, Wolters-Arts M, Feron R, Mariani C, Vriezen WH. The *Solanum lycopersicum* auxin response factor 7 (*Sl* ARF7) regulates auxin signaling during tomato fruit set and development. Plant J. 2009;57:160–70.
84. Benjamins R, Scheres B. Auxin: the Looping Star in Plant Development. Annu Rev Plant Biol. 2008;59:443–65.
85. Leyser O. Dynamic Integration of Auxin Transport and Signalling. Curr Biol. 2006;16:R424–33.
86. Hedden P, Phillips AL. Gibberellin metabolism: new insights revealed by the genes. Trends Plant Sci. 2000;5:523–30.
87. Watanabe D, Takahashi I, Jaroensanti-Tanaka N, Miyazaki S, Jiang K, Nakayasu M, et al. The apple gene responsible for columnar tree shape reduces the abundance of biologically active gibberellin. Plant J. 2021;105:1026–34.
88. Matsuo S, Kikuchi K, Fukuda M, Honda I, Imanishi S. Roles and regulation of cytokinins in tomato fruit development. J Exp Bot. 2012;63:5569–79.
89. Li Z, Shen J, Liang J, Genome-Wide, Identification. Expression Profile, and alternative splicing analysis of the Brassinosteroid-Signaling kinase (BSK) family genes in Arabidopsis. Int J Mol Sci. 2019;20:1138.
90. Love MI, Huber W, Anders S. Moderated estimation of Fold change and dispersion for RNA-seq data with DESeq2. Genome Biol. 2014;15:550.

Publisher's note